博士論文

Effects of inflammatory stimulations on epithelial-mesenchymal transition of tumor cells and tumor malignancy in canine mammary gland tumor

（犬乳腺腫瘍において炎症性刺激が上皮間葉転換と腫瘍の悪性化に及ぼす影響）

齋藤　友睦

Effects of inflammatory stimulations on epithelial-mesenchymal transition of tumor cells and tumor malignancy in canine mammary gland tumor

（犬乳腺腫瘍において炎症性刺激が上皮間葉転換と腫瘍の悪性化に及ぼす影響）

Laboratory of Veterinary Surgery
Graduate School of Agricultural and Life Sciences
The University of Tokyo

東京大学大学院農学生命科学研究科
獣医学専攻博士課程　獣医外科学研究室

平成２２年度入学

齋藤　友睦

Contents

General introduction

Mammary gland tumor (MGT) is one of the most common tumors in female dogs. The survey in a population of over 80,000 insured female dogs indicated that overall-incidence of 111 per 10,000 dog-years was at risk (Egenvall et al., 2005). Approximately a half of all tumors in female dogs is MGT, and a half of MGTs is diagnosed as malignant (Brodey et al., 1983; Gilbertson et al., 1983). Among various types of canine MGTs (cMGTs), inflammatory mammary carcinoma (cIMC) is extremely malignant, due to its high potentials of invasion to surrounding tissues and of metastasis to various organs, including lung, heart, spleen, liver, urinary bladder, lymph node and brain (Clemente et al., 2010a; Kim et al., 2011; Marconato et al., 2009; Peña et al., 2003; Pérez-Alenza et al., 2001). Canine mammary gland carcinoma with inflammatory symptoms is clinically diagnosed as cIMC, and its histopathological feature is the emboli of lymphatic vessels with tumor cells (Fig. 0). Mean survival time in dog with cIMC was about 50 days after diagnosis (Marconato et al., 2009; Pérez-Alenza et al., 2001; Souza et al., 2009).

Dogs with cIMC are similar to cases of human inflammatory breast cancer (hIBC) (Peña et al., 2003). Human IBC is rare but highly aggressive and cancer cells of hIBC also embolized lymphatic vessels in the skin of the breast. Median survival time of hIBC was less than 4 years and the 5-year-survival rate was reported to be 34% in the survey from 1988 to 2001 in U.S.A. (Anderson et al., 2005). The guideline of diagnosis and treatment for hIBC was issued in the

International Conference of Inflammatory Breast Cancer (Dawood et al., 2011). Following the guideline, patients with hIBC are recommended systemic chemotherapy for the primary treatment. If the size of tumor is reduced, then radical mastectomy is performed and following adjuvant radiation therapy is recommended.

In contrast, chemotherapy, surgery and radiation were reported to be less effective for cIMC (Marconato et al., 2009; Souza et al., 2009). Marconato *et al.* reported that the mean survival times of cIMC patients with and without medical treatments were 24 and 80 days, respectively. They also reported the survival times of three cIMC dogs treated surgery were 40, 264 and 278 days, respectively.

The epithelial–mesenchymal transition (EMT) is a complex biological process by which the morphology of polarized epithelial cells is converted to fibroblastic mesenchymal cells. This phenomenon has been known to occur during embryonic development and fibrosis (Lamouille et al., 2014; Nakaya and Sheng, 2013; Thiery et al., 2009). Several cycles of EMT and mesenchymal-epithelial transition (MET), the reverse process of EMT, are essential for final differentiation of internal organ formation (Lamouille et al., 2014; Nakaya and Sheng, 2013; Thiery et al., 2009). During EMT-MET cycle, primary EMT occurs at gastrulation phase; secondary EMT occurs in somites to generate mesenchymal cells with more restricted differentiation potential, and final EMT works on heart development (Thiery, 2002).

Recently, EMT was reported to be involved in cancer invasion and metastasis process (Kalluri and Weinberg, 2009; Tsuji et al., 2009). Induction of EMT is evaluated by the down-regulation of epithelial markers, such as E-cadherin, cytokeratin and ZO-1 (Kalluri and Weinberg, 2009) and by the up-regulation of mesenchymal markers, such as vimentin and fibonectin (Kokkinos et al., 2007; Olmeda et al., 2007). For example, the expression of E-cadherin changes in both degree and localization during EMT, leading to weakened cell-cell adhesion interactions (Morali et al., 2001). Cytokeratin and vimentin were reported to be down-regulated and up-regulated in breast carcinoma patients with micro metastasis, respectively (Willipinski-Stapelfeldt et al., 2005). Localization of ZO-1 was reported to shift from cell surface to cytoplasm and nuclear during EMT (Polette et al., 2007). UP-regulation of fibronectin was reported in breast cancer patients with metastasis (Fernandez-Garcia et al., 2014).

EMT was reported to be regulated by various growth factors and cytokines (Brown et al., 2004; Fernando et al., 2011; Fuxe and Karlsson, 2012; Kamitani et al., 2011; Li et al., 2011; Miettinen et al., 1994; Nicolás et al., 2003; Xu et al., 2009). Among them, transforming growth factor beta (TGF-β) was reported to be one of the key factors that induces EMT with several cell lines (Xu et al., 2009). For instance, TGF-β was reported to induce the morphological change, down-regulation of E-cadherin and up-regulation of fibronectin in mouse mammary gland

epithelial cell (Miettinen et al., 1994). However, TGF-β was also reported to induce EMT only in 2 of the 18 cell lines in one study (Brown et al., 2004). Other factors such as tumor necrosis factor alpha (TNF-α) and interleukin 6 (IL-6), were also reported to induce EMT in some cell lines. TNF-α was reported to induce the morphological change, down-regulation of E-cadherin and up-regulation of vimentin in human prostate cancer cell (Wang et al., 2013a). IL-6 was reported to induce the morphological change, down-regulation of E-cadherin and up-regulation of vimentin in human head and neck tumor cell (Yadav et al., 2011).

Inflammation is also an important factor for tumor progression (Balkwill, 2006; Balkwill and Mantovani, 2001; Diakos et al., 2014; Yang and Wolf, 2009). Inflammatory cytokines were reported to affect tumor progressions in various tumors (Balkwill, 2006; Balkwill and Mantovani, 2001; Ben-Baruch, 2003). Secretions of TNF-α, IL-8 and interleukin 10 (IL-10) were detected from tumor associate macrophages in hIBC patients. These inflammatory cytokines induced morphological changes and promoted migration and invasion in hIBC cell line (Mohamed et al., 2014). Furthermore, gene activations of NF-κB related gene which suggested to be involved in EMT, were reported to be higher in hIBC patients than in non-hIBC (Lerebours et al., 2008). Thus hIBC is thought to have close relationship with inflammation inducing EMT.

Based on above, there formed the hypothesis that inflammation and EMT induced by

inflammation affected the malignancy of cMGT. To prove the hypothesis, the following study was performed. The expressions of EMT markers were compared to evaluate the difference of EMT between cIMC and non-cIMC in chapter 1. In chapter 2, canine recombinant TGF-β, TNF-α and IL-6 were purified and examined their availability for the following study. In chapter 3, six cMGT cell lines were stimulated with canine recombinant proteins to investigate whether EMT was induced (section 1). In section 2 of chapter 3, MGT cell line was cloned for further investigations. The clonal cells which were sensitive to inflammatory stimulations and had the most epithelial-like feartures, were stimulated by cytokines and evaluated for expression changes of EMT markers. In chapter 4, clonal cells which selected in chapter 3 were subcutaneously injected into nude mice and stimulated with cytokines to investigate whether inflammatory stimulations induced EMT and affected tumor malignancy *in vivo*.

(a) (b)

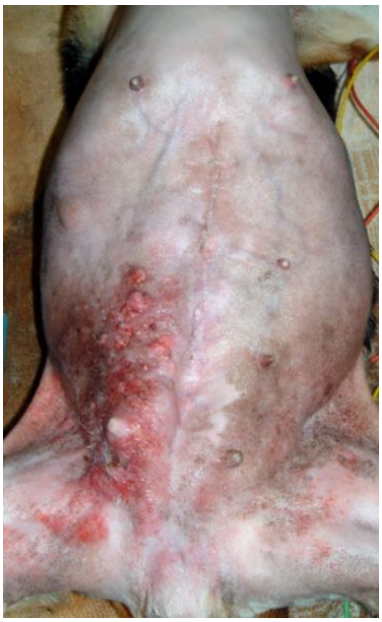

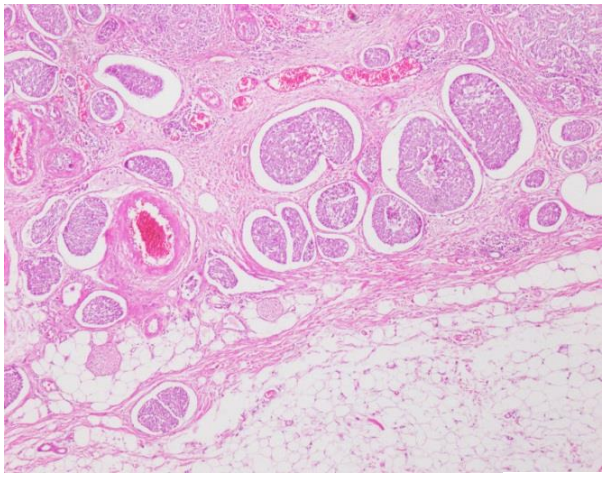

×100

Fig 0 Canine inflammatory carcinoma.

Dogs with cIMC exhibit inflammatory symptoms such as redness, edema, hot feeling and pain (a). The histopathological feature of cIMC is the emboli of tumor cells in lymphatic vessels with hematoxylin-eosin stain (b).

Chapter 1

Evaluation of epithelial-mesenchymal transition in canine inflammatory and non-inflammatory mammary carcinomas

1.1 Introduction

Epithelial-mesenchymal transition (EMT) is a phenomenon that a polarity of cells is lost and the cell morphology is shifted from epithelial to mesenchymal forms (Kalluri and Weinberg, 2009). During EMT, expressions of epithelial and mesenchymal markers such as E-cadherin, cytokeratin, ZO-1, vimentin and fibronectin were shifted (Kalluri and Weinberg, 2009). EMT has been also reported to be involved in cancer invasion and metastasis (Kalluri and Weinberg, 2009; Tsuji et al., 2009). Various types of carcinoma cells were reported to acquire mesenchymal phenotype both *in vivo* and *in vitro* (Bagnato and Rosanò, 2007; Blanco et al., 2004; Chen et al., 2013). At the invasive front of tumor, tumor lost their polarity and expression of E-cadherin was reduced (Brabletz et al., 2001). During the process of metastasis, tumor cells acquired the ability of migration and invasion via EMT and intravasated into blood and lymph vessels (Tsuji et al., 2009). Then, tumor cells were delivered to metastatic regions and reacquired epithelial features for engraftments (Christiansen and Rajasekaran, 2006). Indeed, an ovarian cancer invasion was reported to be promoted via EMT process (Bagnato and Rosanò, 2007), and EMT induced by Twist-1 promoted metastasis of breast tumor cells in mouse (Casas *et al.*, 2011). As mentioned earlier, EMT is closely related to tumor progression and metastasis, and thought to be a key factor of tumor malignancy. Evaluation of EMT progression and elucidation of EMT mechanism may lead to effective therapy for each tumor and make an

improvement of prognosis.

Human breast cancer patients with low E-cadherin and high vimentin expression were reported to show poor prognosis (Liu et al., 2013). Other report indicated that breast cancer patients with low cytokeratin and/or high vimentin showed a tendency of recurrence and metastasis (Vora et al., 2009). Furthermore, reduction of E-cadherin was reported to progress tumor growth, invasion and metastasis in cMGT (Sarli et al., 2004), and expression change of E-cadherin was reported to correlate with malignancy of cMGT (Yoshida et al., 2014). Thus, EMT is thought to relate with the malignant behavior of breast cancer and MGT. Human IBC was reported to secrete TNF-α (Mohamed et al., 2014), one of the EMT inducing factors. Because of the highly metastatic potentials of hIBC, hIBC is supposed to have relationship with EMT. However, the information of EMT in clinical samples of hIBC is limited. Regarding to E-cadherin, it was reported higher expressions of E-cadherin was obseved on the membrane of cancer cells in primary lesions and intralymphatic tumor cells of hIBC patients than of non-hIBC (Charafe-Jauffret et al., 2004; Kleer et al., 2001; Levine et al., 2012). Kleer *et al.* suggested that this E-cadherin expression in primary lesions may decrease during migration from primary lesion to secondary lesion. E-cadherin expression on intralymphatic tumor cells was thought to be one of the possible causes about emboli of dermal lymph vessels (Fernandez et al., 2013; Morales and Alpaugh, 2009). Expressions of other EMT markers in hIBC tissues

were still unclear. Canine IMC have severe clinical features and show rapid progression and metastasis (Clemente et al., 2010a; Kim et al., 2011; Marconato et al., 2009; Peña et al., 2003; Pérez-Alenza et al., 2001). Expression of vimentin was reported in cIMC (Clemente et al., 2010b), but the information of EMT in cIMC is also limited.

The purpose of this chapter was to investigate EMT in cIMC in comparison to non-cIMC by evaluating the expressions of epithelial and mesenchymal markers.

1.2 Materials and Methods

1.2.1 Clinical cases with mammary carcinoma

Tissue specimens of cIMC and non-cIMC were used for this study. The diagnosis of cIMC was made by finding of embolized tumor cells in lymph vessels (Marconato et al., 2009; Pérez-Alenza et al., 2001). Canine IMC samples were kindly provided from following institutes; Laboratory of Veterinary Pathology, Graduate School of Agriculture and life Sciences, The University of Tokyo, Tokyo, Japan; Laboratory of Veterinary Pathology, Department of Veterinary Science, Osaka Prefecture University, Osaka, Japan; Laboratory of Veterinary Pathology, Department of Veterinary Medicine, Nippon Veterinary and Life Science University, Tokyo, Japan, and North lab, Hokkaido, Japan. Non-cIMC samples were collected from The Veterinary Medical Center, The University of Tokyo. Tumor tissues of cIMC were classified into tubulopapillary carcinoma (n=17), and tumor tissues of non-cIMC were classified into tubulopapillary carcinoma (n=19) and complex carcinoma (n=6) according to the International Histological Classification of Tumors of Domestic Animals of the World Health Organization (Misdorp et al., 1999). Age, breed and regional lymph node involvement of patients were obtained from clinical records of these institutes.

1.2.2 Antibodies

For immunohistochemistry, mouse anti-E-cadherin (BD Biosciences, NJ, USA), rabbit anti-ZO-1 (Santa Cruz Biotechnology, CA, USA) and mouse anti-cytokeratin 18 (Abcam, Cambridge, UK) were used as primary antibodies of epithelial markers. The primary antibodies used for mesenchymal markers were mouse anti-vimentin (Dako Japan, Kyoto, Japan) and rabbit anti-fibronectin (Dako Japan).

The primary antibodies for immunofluorescence were rabbit anti-E-cadherin (Cell Signaling Technology, MA, USA) and anti-vimentin (Millipore, MA, USA). Fluorescein goat anti-rabbit IgG (H+L) (Life technologies, MA, USA) and Alexa Fluor 568 goat anti-mouse IgG (H+L) (Life technologies) were used for the secondary antibodies for immunofluorescent staining.

1.2.3 Immunohistochemistry

Formalin-fixed paraffin-embedded sections were deparaffinized, and then antigen epitope was retrieved by appropriate methods (Table 1.1). After epitope retrieval, to inactivate the endogenous peroxidase sections were incubated in 0.3% hydrogen peroxide in methanol for 10 minutes at 4°C with light interception. Then nonspecific protein bindings were blocked using 0.1 % Tween 20 in phosphate buffered saline (PBST) containing 5 % normal goat serum (Sigma

Aldrich, MO, USA) for 1 hour at room temperature. Sections were incubated with primary antibodies with the conditions listed in Table 1.1. After incubation, sections were treated with polymer solution containing HRP-conjugated antibody against mouse immunoglobulin for E-cadherin, vimentin and cytokeratin 18, and against rabbit immunoglobulin for ZO-1 and fibronectin, respectively. Visualizations were done by liquid DAB/hydrogen peroxidase solution (Dako) with proper durations (Table 1.1). Nuclear counter staining was performed using by Mayer's hematoxylin solution.

1.2.4 Immunofluorescent double staining

The overview of the conditions was shown in Table 1.2. Protocols of epitope retrieval were same as those of immunohistochemistry. Then nonspecific protein bindings were blocked using PBST containing 5 % normal goat serum for 1 hour at room temperature. Sections were incubated with primary antibodies simultaneously at 4°C over-night. After incubation, sections were incubated with secondary antibodies simultaneously for 1 hour at room temperature under light interception. Then, slides were mounted in DAPI containing Vectashield mounting medium (Vector Laboratories, CA, USA). Fluorescent images were scanned by LSM 700 (Carl Zeiss, Oberkochen, Germany).

1.2.5 Evaluation of EMT

The immunohistochemical slides were examined in the blind of histological diagnosis. A total of 3 random fields (200x) were selected from tumor region to evaluate the expressions of epithelial and mesenchymal markers (EMT markers). Epithelial markers used in this chapter were E-cadherin, cytokeratin 18 and ZO-1. Mesenchymal markers used in this chapter were vimentin and fibronectin.

In the samples of immunohistochemistry, positive tumor cells for EMT markers were counted and positive rates of each EMT marker were calculated. EMT was evaluated by the change rate of EMT marker expression. The change rate considered as EMT was reported to be from 1 percent to 25 percent (Sarli et al., 2004; Willipinski-Stapelfeldt et al., 2005; Yoshida et al., 2014). In this study, five percent was set as cut off value to avoid the influence of false negative and false positive. For epithelial markers, positive rate of less than 95% was considered to be a loss of epithelial marker. For mesenchymal markers, positive rate of more than 5% was considered to be an emergence of mesenchymal markers. In this study, these changes were defined as EMT changes. EMT status of each case was expressed as an accumulation of EMT changes of five EMT markers scored as 0-5; Change of one marker was counted as 1.

In immunofluorescent staining samples, co-localization of E-cadherin and vimentin

was evaluated in three fields (200x) by confocal laser scanning microscopy. Cells numbers were counted according to their expression pattern of E-cadherin and Vimentin.

1.2.6 Statistical analysis

Statistical analyses of expression rates of epithelial and mesenchymal markers and EMT status were performed using Student's t-test. The relationship between each two EMT markers was analyzed by Spearman's rank-correlation coefficient. A chi-square test was used to evaluate the associations between EMT change of each marker and lymph node metastasis. Values of $p < 0.05$ were considered statistically significant.

1.3 Results

1.3.1 Clinical cases with mammary carcinoma

Total of 42 dogs diagnosed as cIMC and non-cIMC from 1996 to 2013 were included in this study. Case number of cIMC and non-cIMC was 17 and 25, respectively. Clinical data of these cases was shown in Table 1.3. The ratio of lymph node metastasis in dogs with cIMC was significantly higher than in dogs with non-cIMC ($p < 0.01$). Breeds of cIMC cases included 6 Miniature Dachshund, 3 Shih Tzu, 2 Shiba, Cavalier King Charles Spaniel, Welsh Corgi, Miniature Schnauzer, Chihuahua and 2 mongrel. Breeds of non-cIMC were as follows; 7 Maltese, 3 Shetland Sheepdog, 2 Shih Tzu, 2 Miniature Dachshund, 2 Toy Poodle, Labrador Retriever, Siberian Husky, Pug, Pomeranian, Italian Greyhound, Papillon and 3 mongrel.

1.3.2 Expression of EMT markers and EMT status

Positive rates of EMT markers in cIMC and non-cIMC cases were shown in Fig 1.1 and Fig 1.2. Based on positive rates of EMT markers, EMT changes were evaluated and representative figures were shown in Fig. 1.3. Table 1.5 showed the ratio of cases which exhibited EMT change of each EMT markers. Significantly higher percentages of EMT changes such as E-cadherin, vimentin and fibronectin were observed in cIMCs than in non-cIMCs, thought changes of cytokeratin 18 and ZO-1 were similar in both cases ($p < 0.01$). EMT change

of vimentin had a relationship with lymph node metastasis in cIMC ($p < 0.01$). The result of EMT status which obtained by scoring of EMT changes was shown in Table 1.6. An average of EMT status of cIMC cases was significantly higher than that of non-cIMC cases ($p < 0.01$) (Table 1.6).

Expression of fibronectin was increased in cIMCs ($p < 0.01$). On the contrary, expression of cytokeratin 18 was significantly reduced in non-cIMCs ($p < 0.01$). To evaluate the relationship between each EMT markers, correlations of coefficient were calculated, but no correlation was observed among EMT markers both in cIMC and non-cIMC cases (Table 1.4).

1.3.3 Co-localization of E-cadherin and Vimentin

Expression pattern of E-cadherin and vimentin were varied among cells (Fig 1.4). All cells were classified into 5 groups according to the expression degree and localization; E-cadherin(++)/vimentin(+), E-cadherin(++)/vimentin(-), E-cadherin(+)/vimentin(+), E-cadherin(+)/vimentin(-) and E-cadherin(-)/vimentin(+) (Fig 1.4). Among these classifications, number of E-cadherin negative and vimentin positive cells of cIMC cases was significantly higher than that of non-cIMC cases ($p < 0.01$) (Fig 1.5).

1.4 Discussion

In this chapter, total of 17 cases of cIMC tissue samples was examined to investigate the relationship between EMT and cIMC comparing with 25 cases of non-cIMC. Canine IMC contained only tubulopapillary carcinoma in this study, whereas Clemente *et al.* reported that although approximate 60 percent of cIMC were involved in tubulopapillary carcinoma, cIMC also contained solid carcinoma, anaplastic carcinoma lipid-rich carcinoma and carcinosarcoma (Clemente et al., 2010a). This difference may come from small number of cases. Ages and sizes of dogs did not show significant difference between cIMC and non-cIMC cases. The ratio of large breeds with cIMC was about 25% in this study. The total of 127 female dogs was reported to diagnosed as cIMC and a half of them was large breed (Clemente et al., 2010a; Marconato et al., 2009; Peña et al., 2003; Pérez-Alenza et al., 2001; Souza et al., 2009). The ratio of large breeds with cIMC in this study was low comparing to those investigated in foreign countries, which was thought to reflect the low number of large breeds in Japan. Although large breeds were reported to be more affected with malignant MGT compared with small breeds in dogs (Itoh et al., 2005), the ratio of large breed was almost same in both cIMC and non-cIMC in this study. This result may indicate that the risk of onset of cIMC was not difference between large and small breeds. In addition, the age of onset was similar between cIMC and non-cIMC. It may indicate that tumorigenesis of cIMC and non-cIMC is similar in their onset. After onset of

carcinoma, some kind of factors may make differences between the tumor progression of cIHC and non-cIHC.

EMT in both cIMC and non-cIMC was evaluated by scoring of expression changes of EMT markers; down-regulations of epithelial markers and up-regulations of mesenchymal markers in specimen. The average score of EMT change in cIMC was significantly higher than in non-cIMC. As the average score represents cumulative numbers of changed EMT markers per case, higher average in cIMC was thought to suggest closer relationship between EMT and cIMC than non-cIMC. Regarding to each EMT marker expression, the ratio of changes in 3 EMT markers, E-cadherin, vimentin and fibronectin, were higher in cIMCs than in non-cIMCs. Similarly, there were significantly higher ratio of E-cadherin(+)/Vimentin(-) cells which were considered to be progressing in EMT in cIMC than in non-cIMC. Although lymph node remarks were limited in this study, obtain of vimentin was supposed to be associated with lymph node metastasis. Furthermore, the positive cell rate of fibronectin was significantly higher in cIMC than in non-cIMC. These three EMT markers were reported to be related to tumor proliferation, invasion and metastasis in cMGT (Peña et al., 1994; Rismanchi et al., 2014; Sarli et al., 2004). Therefore, there was a possibility that these EMT marker changes were related to the higher malignancy of cIMC. On the other hand, the positive cell rate of cytokeratin 18 was significantly lower in non-cIMC than in cIMC, although EMT changes in this marker had been

observed in both groups. Reduction of cytokeratin 18 expression was reported to be related to proliferation of tumor and to be related with poor prognosis in human breast cancer (Willipinski-Stapelfeldt et al., 2005; Woelfle et al., 2004).. Because tissue samples investigated in this study were diagnosed as malignant, EMT change in cytokeratin 18 observed in both groups may be associated with their malignancy. Although cytokeratin 18 was reported to participate in oncogenic transformation, cell proliferation and apoptosis through various signaling pathway, the role of cytokeratin 18 in tumor was still unclear (Weng et al., 2012) Further investigation of consequence of difference in cytokeratin 18 expression rates between cIMC and non-cIMC including the search of relative factors and prognostic data was needed.

EMT was suggested to occur and proceed in cIMC comparing to non-cIMC, whereas relationship between EMT and clinical data was not observed in this study. This might be caused by small number of cases. In addition, clinical and prognostic data were not sufficiently obtained in this study, because samples and clinical data were collected from multiple institutes. Large scale survey was needed to clarify the relationship between EMT on cIMC and clinical and prognostic data.

In this chapter, cIMC showed closer relationship with EMT in comparison to non-cIMC. Malignancy of cIMC such as rapid growth and metastasis was suggested to relate to EMT. To reveal the relationship between EMT and cIMC, further extensive studies both *in vitro*

and *in vivo* was thought to be needed. Induction of EMT by several cytokines in cMGT cell lines and evaluation of EMT changes were performed in following chapter.

Table 1.1 Protocols for immunohistochemistry.

Primary antibody	Antigen-retrieval	Reaction condition	DAB[3]
E-cadherin	121ºC, 5 min in CB[1]	1:150, 4ºC, over-night	RT[2], 3 min
Vimentin	121ºC, 5 min in CB[1]	1:50, 37ºC, 1 h	RT[2], 1 min
Cytokeratin18	121ºC, 5 min in CB[1]	1:500, 4ºC, over-night	RT[2], 2 min
ZO-1	121ºC, 5 min in CB[1]	1:100, 4ºC, over-night	RT[2], 3 min
Fibronectrin	RT[2], 5 min, in proteinase K	1:1000, 37ºC, 50 min	RT[2], 50 sec

[1]CB, 10mM sodium citrate buffer, pH6.0

[2]RT, room temperature

[3]DAB, 3, 3'-diaminobenzidin/hydrogen peroxide solution

Table 1.2 Protocols for immunofluorescent double staining.

Primary antibody	Antigen-retrieval	Reaction condition	Secondary antibody	Reaction condition
E-cadherin	121ºC, 5 min in CB[1]	1:300, 4ºC, over-night	Fluorescein anti rabbit IgG	1:300, RT[2], 1 h
Vimentin	121ºC, 5 min in CB[1]	1:500, 4ºC, over-night	Alexa Fluor 568 anti mouse IgG	1:300, RT[2], 1 h

[1]CB, 10mM sodium citrate buffer, pH6.0

[2]RT, room temperature

Table 1.3 Clinical data of cIMC and non-cIMC patients.

Clinical data			
Historogical diagnosis			n=42
	cIMC		
		Tubulopapillary carcinoma	17(100%)
	non-cIMC		
		Tubulopapillary carcinoma	19(76%)
		Complex carcinoma	6(24%)
Age(years)			
	mean		
		cIMC	11.5±2.3
		non-cIMC	11.7±2.1
	median		
		cIMC	12
		non-cIMC	11.5
Breed			
	cIMC		
		small	11(64.7%)
		large	4(23.5%)
		mongrel	2(11.8%)
	non-cIMC		
		small	17(68.0%)
		large	5(20.0%)
		mongrel	3(12.0%)
Lymph node metastasis			
	cIMC		11/12(91.7%) *
	non-cIMC		6/16(37.5%)

*: $p < 0.01$

Table 1.4 Correlations of EMT markers.

cIMC	Correlation of coefficient				
	E-cadherin	Vimentin	Cytokeratin18	ZO-1	Fibronectin
E-cadherin	-	-0.33	0.38	-0.25	0.11
Vimentin		-	-0.27	0.14	0.27
Cytokeratin18			-	0.27	0.23
ZO-1				-	0.39
Fibronectin					-

non-cIMC	Correlation of coefficient				
	E-cadherin	Vimentin	Cytokeratin18	ZO-1	Fibronectin
E-cadherin	-	-0.16	0.36	-0.14	0.22
Vimentin		-	-0.15	-0.19	0.14
Cytokeratin18			-	0.10	0.38
ZO-1				-	-0.00
Fibronectin					-

Table 1.5 Number of cases which showed EMT change of each EMT markers in cIMC and non-cIMC groups.

	The ratio of cases which exhibit EMT change (%)				
	E-cadherin	Vimentin	Cytokeratin18	ZO-1	Fibronectin
cIMC	59*	88 *	100	29	100*
non-cIMC	20	36	100	28	72

*: $p < 0.01$

Table 1.6 EMT status of cIMC and non-cIMC cases.

	EMT status						
	0	1	2	3	4	5	Average
cIMC (n=17)	0	0	0	6	9	2	3.76 *
non-cIMC (n=25)	0	3	10	8	3	1	2.56

*: $p < 0.01$

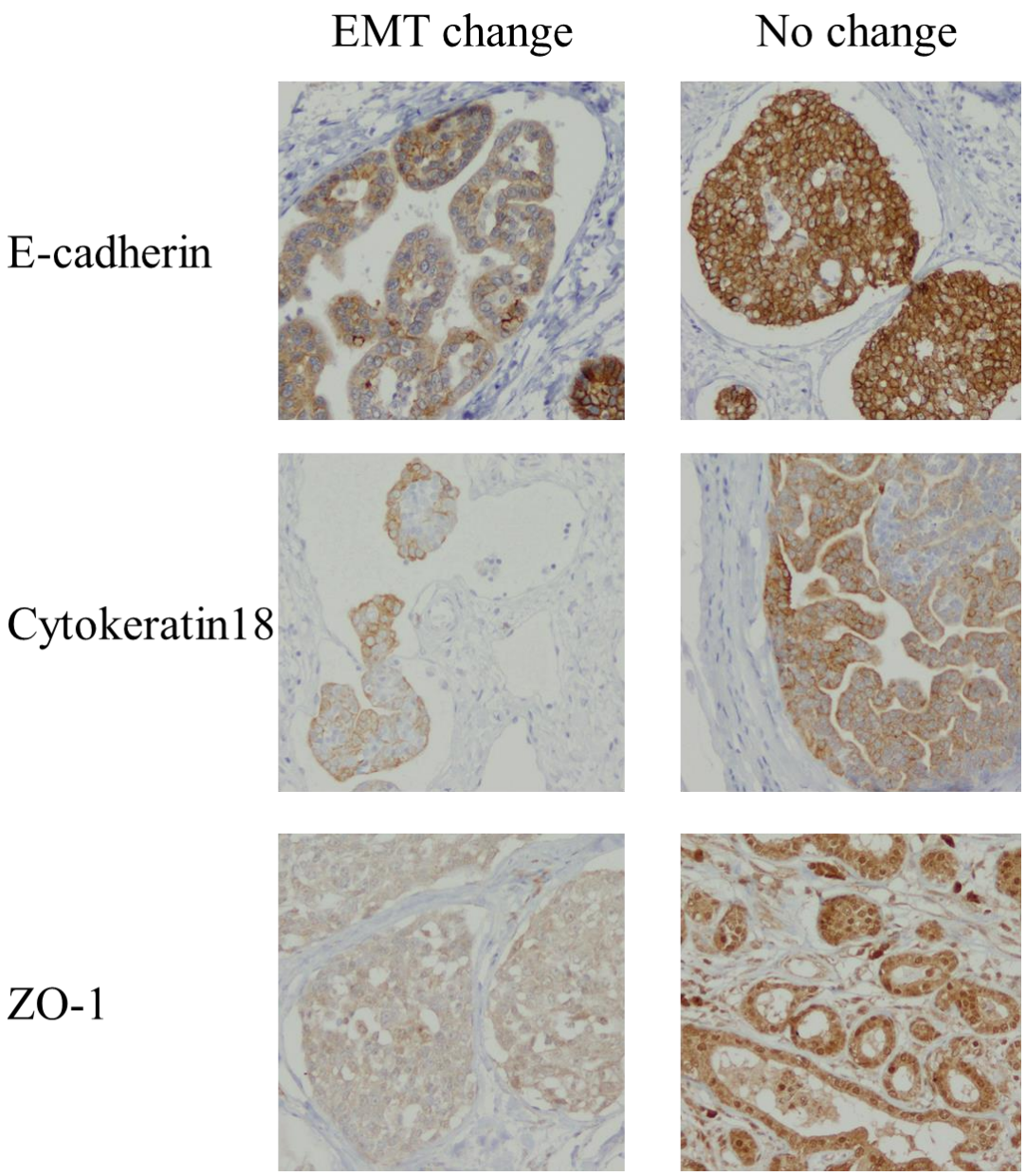

Fig 1.1 EMT changes based on the expressions of epithelial markers.

For epithelial markers (E-cadherin, cytokeratin 18 and ZO-1), positive rate of under 95% in average of tumor cells was determined as EMT change.

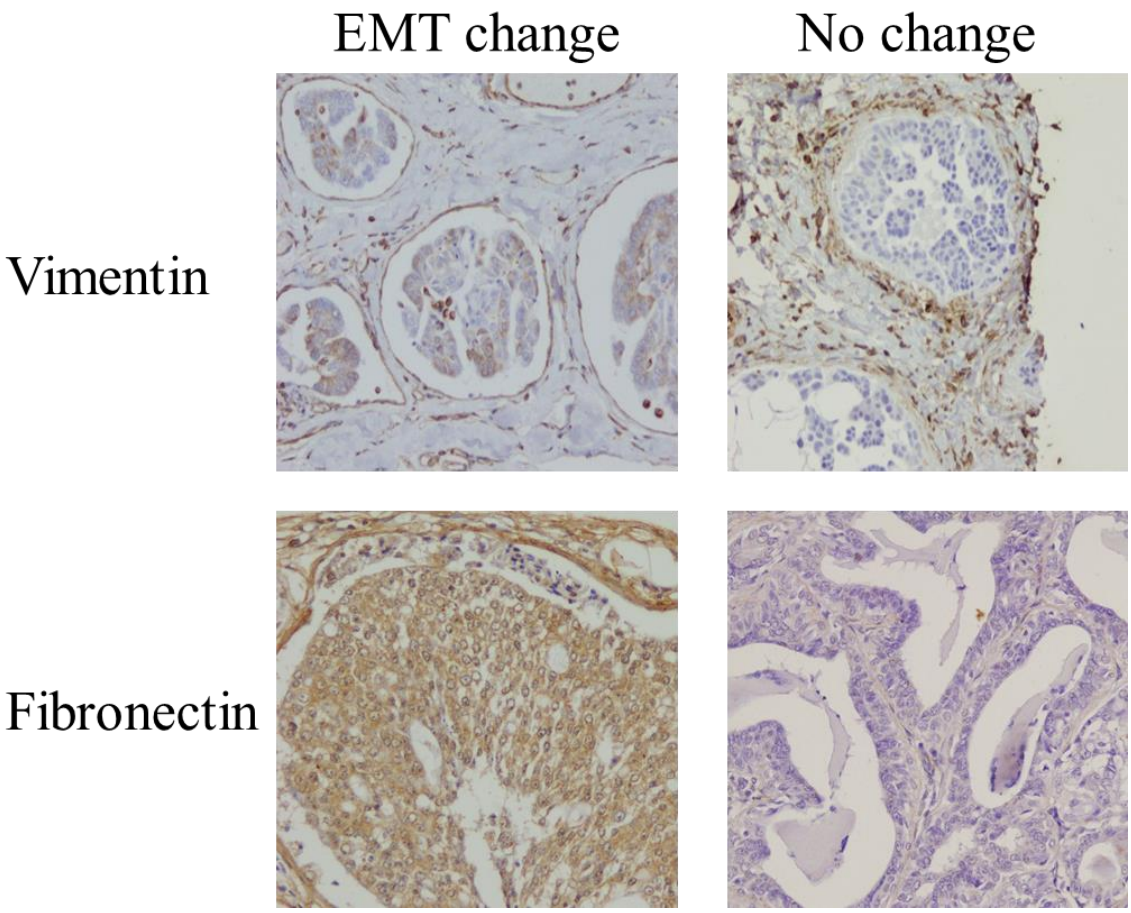

Fig 1.2 EMT changes based on the expressions of mesenchymal markers.

For mesenchymal markers (vimentin and fibronectin), positive rate of over 5% in average was defined as EMT change.

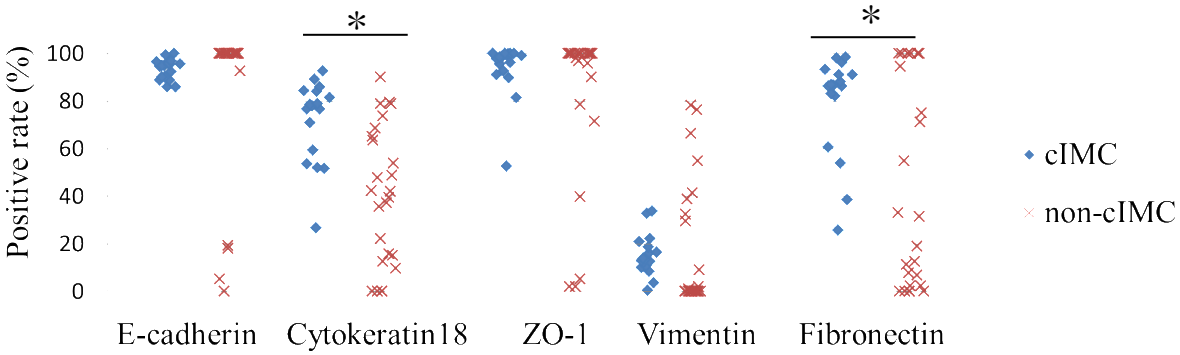

Fig 1.3 Positive rate of EMT markers' expression.

Positive rates of both epithelial and mesenchymal markers were plotted. The reduction of cytokeratin18 expressions was significantly higher in non-cIMC than in cIMC. The expression rate of Fibronectin was significantly higher in cIMC than in non-cIMC.

＊: $p < 0.01$.

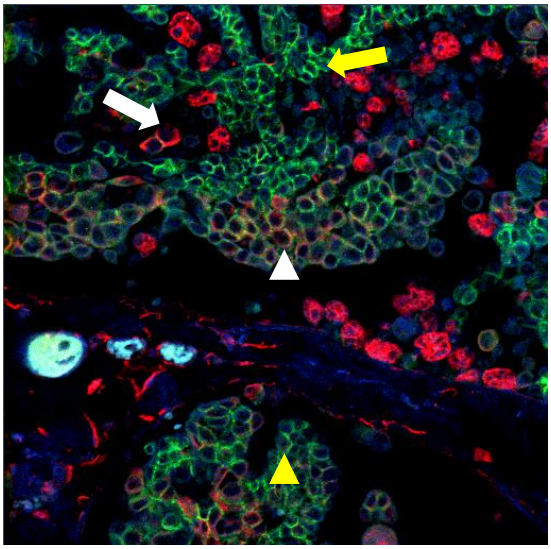

(×200)

Fig 1.4 Expression and localization of E-cadherin and Vimentin.

Figure showed a representative image (×200) of double staining with E-cadherin (green) and vimentin (red) on cIMC cells. Expression pattern was varied among cells; strong expression of E-cadherin and no expression of vimentin (yellow arrow), weak expression of E-cadherin and no expression of vimentin (yellow arrowhead), no expression of E-cadherin and expression of vimentin (white arrow) and weak expression of E-cadherin and expression of vimentin (white arrowhead). Green: E-cadherin. Red: Vimentin. Blue: DAPI.

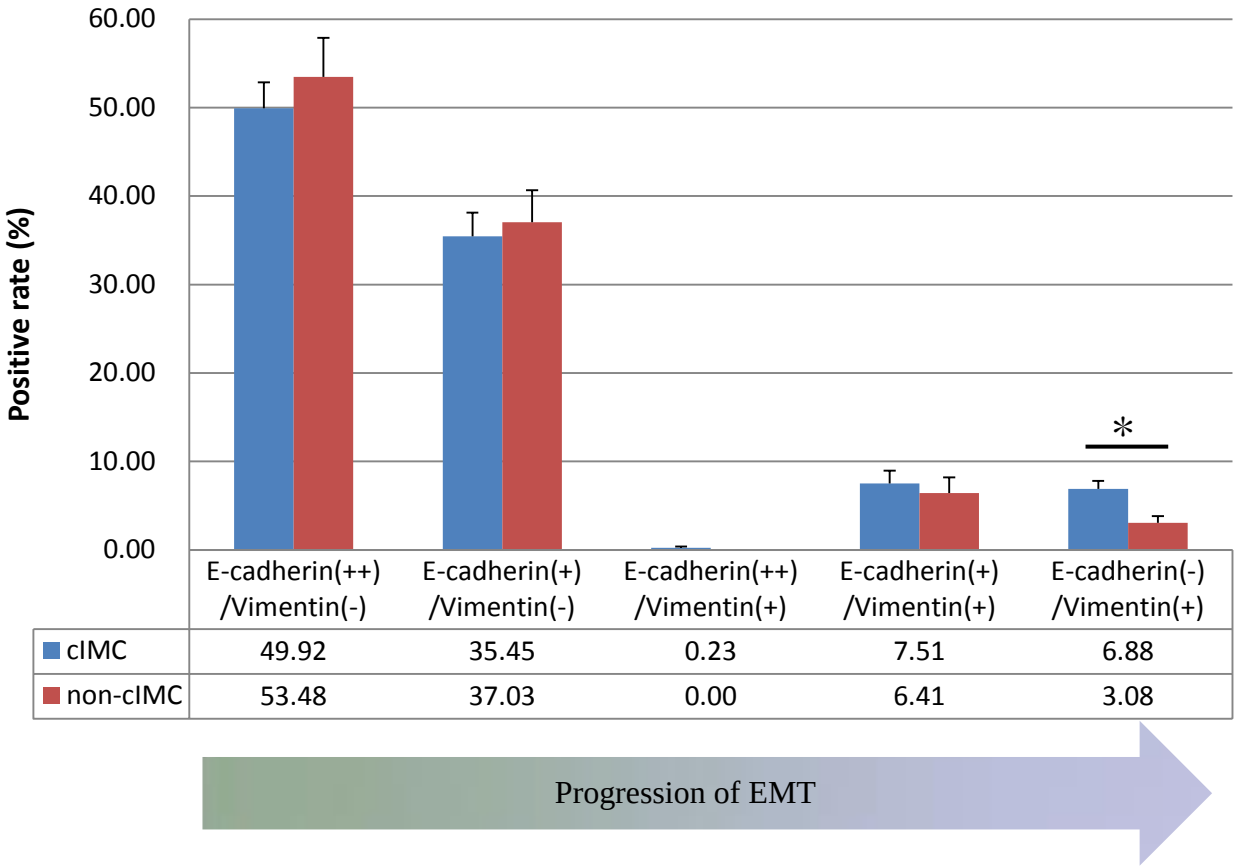

Fig 1.5 Co-localizations of E-cadherin and Vimentin.

Co-localizations of E-cadherin and vimentin were evaluated. The rate of E-cadherin negative and vimentin positive cells (E-cadherin(-)/Vimentin(+) cells) was significantly higher in cIMC cases than in non-cIMC cases.

＊: $p < 0.01$. Vertical bar represents SE.

Chapter2

Investigation of the ability of canine recombinant inflammatory cytokines to induce EMT in MDCK cells

2.1 Introduction

In the previous chapter, cIMC showed stronger EMT change in comparison to non-cIMC. EMT has been reported to be regulated by various growth factors and cytokines (Brown et al., 2004; Fernando et al., 2011; Fuxe and Karlsson, 2012; Kamitani et al., 2011; Li et al., 2011; Miettinen et al., 1994; Nicolás et al., 2003). For example, TGF-β induced EMT in mouse mammary gland epithelial cells (Miettinen et al., 1994). In this report, morphological change and reduction of E-cadherin and ZO-1 were reported. Co-stimulation of TGF-β and TNF-α was reported to induce morphological change and vimentin expression in bronchial epithelial cells (Kamitani et al., 2011). IL-6 was reported to induce morphological change and expression change of E-cadherin and vimentin in head and neck tumor cell (Yadav et al., 2011). As cIMC exhibits inflammatory clinical signs, EMT in cIMC was thought to be affected by these factors, especially inflammatory cytokines. For further investigation of relationship between malignancy of cMGT and inflammation inducing EMT, it is important to reveal the role of inflammatory cytokines during EMT.

In veterinary medicine, human recombinant TGF-β is known to induce EMT in Madin-Darby canine kidney (MDCK) cells (Moyano et al., 2010; Zhang et al., 2006), but it remains unclear whether inflammatory cytokines can induce EMT in this cell line. Cross reactivity of cytokines differed with each cytokines (Just et al., 1991; Vieira et al., 1991).

Additionally, homology between human gene and canine gene of these cytokines is not so high. To investigate EMT in dogs accurately, construction and purification of canine recombinant cytokine was thought to be needed.

The purpose of this chapter was to construct and purify canine recombinant TGF-β, TNF-α and IL-6 for the studies of following chapter. Their effects of EMT induction on MDCK cells were evaluated by changes of E-cadherin expression and cell morphology.

2.2 Materials and methods

2.2.1 Cell culture

MDCK cells were kindly provided by Associate Professor Horimoto at the University of Tokyo and were cultured in Dulbecco's modified Eagle's medium (DMEM; Wako, Osaka, Japan) containing 5% fetal bovine serum (FBS). Canine mammary gland tumor cell line, CHMp (Uyama et al., 2006), cells were cultured in RPMI1640 containing 10% FBS. These cells were maintained in a humidified atmosphere of 5% CO_2 at 37°C.

2.2.2 RNA isolation

Canine RNA was extracted from CHMp cells using TRI Reagent (Molecular Research Center Inc., OH, USA) according to the manufacturer's instructions. Canine macrophage RNA was kindly provided by Professor Tsujimoto at the University of Tokyo (Goto-Koshino et al., 2011).

2.2.3 Expression and purification of cTGF-β, cTNF-α, and cIL-6

cDNA of cTGF-β was amplified by reverse transcription-polymerase chain reaction (RT-PCR) from canine RNA extracted from CHMp cells using SuperScript III Reverse Transcriptase (Invitrogen, CA, USA). The cDNA of cTNF-α and cIL-6 were amplified from

canine RNA extracted from canine macrophages. Primers used in this study are listed in Table2.1. Amplified cDNA fragments were cloned into a pGEX-6p-2 vector (GE Healthcare, NJ, USA). *Escherichia coli* BL21 (DE3) cells were grown at 25°C, and protein expression of the recombinant plasmids was induced by the addition of 0.1 mM isopropyl-β-D-thiogalactopyranoside (IPTG). For GST and LPS residual control, a pGEX-6p-2 vector alone and no vector control were transfected with *E. coli* BL21 cells. *E. coli* BL21 cells were harvested by centrifugation, resuspended, and sonicated in a sonication buffer (40 mM Tris-HCl, pH 7.5, 150 mM NaCl, 5 mM EDTA, and 0.5% Triton X-100). Recombinant proteins were purified by affinity chromatography using Glutathione-Sepharose 4 beads (GE Healthcare). Proteins bound to the beads were washed with and resuspended in cleavage buffer (50 mM Tris-HCl, pH 7.5, 150 mM NaCl, 1 mM EDTA, and 1 mM dithiothreitol (DTT)). Next, Pre Scission protease (GE Healthcare) was added and the suspension was incubated overnight at 4°C. After centrifugation, the first supernatant was collected. Collected supernatants were dialyzed against phosphate-buffered saline (PBS). Recombinant proteins were detected by western blot analysis. Briefly, solutions of recombinant proteins were used in a mixture of sample buffer (100 mM Tris-HCl, pH6.8, 2% sodium dodecyl sulfate (SDS), 12% 2-mercaptoethanol, 20% glycerol, and bromophenol blue). Samples were run on 4–15% Mini-PROTEAN TGX gel (Bio-Rad Laboratories, CA, USA) and transferred to polyvinylidene fluoride (PVDF)

membranes (Bio-Rad). The membranes were then incubated with rabbit anti-TGF-β_1 (1:1000; LifeSpan Biosciences Inc., WA, USA), rabbit anti-TNF-α (1:500; Abgent, CA, USA), and goat anti-canine IL-6 (1:1000; R&D systems, MN, USA), followed by incubation with anti-mouse IgG conjugated to horseradish peroxidase (HRP) (1:10,000; GE Healthcare), anti-rabbit IgG conjugated to HRP (1:10,000; GE Healthcare), and anti-goat IgG conjugated to HRP (1:100,000; Santa Cruz Biotechnology). Signals were detected using the Luminata Forte Western HRP substrate (Millipore). The experiment was approved by the Life Science Committee of the Graduate School of Agricultural and Lifesciences, the University of Tokyo. (Accession number: 541-2323)

2.2.4 Cell stimulation

Recombinant cTGF-β, cTNF-α, cIL-6, and GST residues were added to the cells at a final concentration of 10 ng/mL and residual LPS control was added at the same dilution of cIL-6, minimum dilution ratio. Cells were incubated at 37 °C for 24 h. Cells were lysed in Triton X-100 buffer (0.5% Triton X-100, 2.5 mM EDTA, 5 mM $MgCl_2$, and 50 mM PIPES; pH 6.2) and collected as soluble fractions. Insoluble cell fractions were washed twice with Triton X-100 buffer and then extracted in buffer containing 1% SDS.

2.2.5 Immunoblot analysis

Cell lysates in sample buffer were used for immunoblot analysis. Samples containing 10 µg of total protein per lane were subjected to gel electrophoresis and transferred to PVDF membranes as described above. The membranes were then incubated with mouse anti-E-cadherin antibody (1:2000; BD Biosciences) and mouse anti-actin antibody (1:10,000; Millipore), followed by incubation with anti-mouse IgG conjugated to HRP. Signals were detected as described above. Quantifications of signals were performed by using ImageJ software.

2.2.6 Immunofluorescent staining

MDCK cells were stimulated as described in section 2.2.4, and incubated for 6 h and 24 h. Cells were fixed with 4% paraformaldehyde (PFA) in PBS and blocked with PBS containing 10% bovine serum albumin for 1 h. Next, cells were incubated with anti-E-cadherin antibody for 1 h, followed by incubation with Alexa 568-conjugated goat anti-mouse IgG antibodies (Invitrogen) for 30 min at room temperature. Cells were then washed three times with PBS and mounted in DAPI containing Vectashield mounting medium (Vector Laboratories).

2.2.7 Cell morphology

MDCK cells were starved for 24 h, followed by stimulation with recombinant cTGF-β, cTNF-α, and cIL-6 at a final concentration of 10 ng/mL in DMEM containing 0.1% FBS, and incubated at 37°C for 6 days. Cells were fixed with 4% PFA in PBS and stained with Wright-Giemsa stain.

2.3 Results

2.3.1 Purification of cTGF-β, cTNF-α, and cIL-6

Recombinant cTGF-β, cTNF-α, and cIL-6 were expressed by *E. coli* (BL21) cells and purified by using Glutathione-Sepharose 4 beads and Pre Scission protease. After cleavage of GST fusion recombinant proteins using Pre Scission protease, recombinant cTGF-β, cTNF-α, and cIL-6 were isolated (Fig. 2.1). These cytokines were used in the following experiments.

2.3.2 Transition of localization and reductions of E-cadherin expressions

At 6 h post-stimulation (p.s.), expression of E-cadherin levels in the insoluble fractions were reduced, whereas increased in the soluble fractions except for the stimulation followed by TGF-β stimulation. This may represent a shift in the localization of E-cadherin. At 12 h p.s., changes in expression patterns were observed in soluble fractions. At 24 h p.s., the total amounts of E-cadherin were reduced under all conditions. In addition, co-stimulation caused significant down-regulation of E-cadherin expression (Fig. 2.2).

Immunofluorescent staining also showed that inflammatory cytokines induced a reduction in cell surface E-cadherin (Fig. 2.3). Co-stimulation enhanced this phenomenon, particularly following TGF-β /IL-6 stimulation. GST residues and residual LPS had no effect on E-cadherin expression (date not shown).

2.3.3 Effects of TNF-α on morphology of MDCK cells

The morphological change from epithelial to mesenchymal form is one of the most essential features of EMT. In this study, cell stimulation induced a decrease in adhesion molecules at 24 h after stimulations, but no changes in cell morphology were observed at 24 h. However, 6 days after stimulations, morphological changes had occurred. TGF-β and IL-6 did not induce the change of cell shape, but TNF-α and TGF-β/TNF-α induced significant morphological changes from cobble to spindle forms, and weakened cell-cell adhesion interactions (Fig. 2.4). GST residues and residual LPS also had no effect on cell morphology (date not shown).

2.4 Discussion

Most cell stimulation studies on canine cells were carried out using human recombinant proteins (Morita et al., 2007; Wang et al., 2013b; Zhang et al., 2006, 2014). However, the homology level between human and canine RNA is not high; homology levels between TGF-β, TNF-α, and IL-6 RNA are 92%, 91%, and 76%, respectively. Because the effects of these disparities were unclear, construction of recombinant proteins derived from dogs, cTGF-β, cTNF-α, and cIL-6, was thought to be needed for evaluating EMT in canine cells correctly.

In this study, cTGF-β, cTNF-α, and cIL-6 were expressed by *E. coli* (BL21) cells and purified successfully. Purified cTGF-β, cTNF-α, and cIL-6 were detected by western blot analysis at 13 kDa, 17kDa and 21 kDa, respectively. The possibility of contamination of minor residual LPS and GST in purified cytokines existed, because these cytokines were expressed by *E. coli* (BL21) cells using pGEX-6p-2 vector which contained GST coding region. These residual LPS and GST did not affect MDCK cells. These cytokines successfully induced EMT change in MDCK cells with the concentration of 10 ng/mL. In the pilot study, 1 ng/mL of cTGF-β did not induce E-cadherin reduction but 10 ng/mL of cTGF-β sufficiently reduced E-cadherin expression. Therefore, these cytokines were suitable for cell stimulations and stimulations were performed at 10 ng/mL.

The results obtained in this chapter indicated that the down-regulation and the shift of E-cadherin were induced not only by TGF-β, but also by inflammatory cytokines, TNF-α and IL-6. E-cadherin was reported to shift its localization from membrane to cytoplasm during EMT (Morali et al., 2001). These three recombinant cytokines were suggested to induce EMT in MDCK cell. The loss of cell surface E-cadherin was caused by cTGF-β/cTNF-α co-stimulation and cTGF-β/cIL-6 co-stimulation at six and twenty four hours post-stimulation, whereas single stimulation by cTGF-β, cTNF-α and cIL-6 caused little changes of cell surface E-cadherin expressions at these time points. Furthermore, cTNF-α stimulation and cTGF-β/cTNF-α co-stimulation induced morphological change of MDCK cells. Co-stimulation of TGF-β and inflammatory cytokines such as TNF-α and IL-6 were reported to enhance morphological change and expression change of E-cadherin in lung cancer cell lines (Abulaiti et al., 2013; Kawata et al., 2012). TGF-β and inflammatory cytokines were suggested to interact with each other and enhance the functions of EMT inducing factors. Thus, the inflammatory cytokines were thought to be not only inducer of EMT but also enhancer of EMT induced by other inducing factor.

Loss or reduction of E-cadherin and morphological change of cells were some features of EMT. Although these three recombinant cytokines showed partials of EMT phenomena, these were thought to be EMT inducible factors. Therefore, in the following chapter, EMT in cMGTs

was investigated *in vitro* and *in vivo* using these cytokines.

Table 2.1 Gene information and primer sequences.

Recombinant protein	Accession number	Primer sequence	Primer position	Length of PCR fragment
cTGF-β	L34956.1	5′- CG*GAATTC* CCGCCCTGGACACCAACTA -3′	892-908	239bp
		5′- ACGC*GTCGAC* TCAGCTGCACTTGCAGGA -3′	1213-1230	
cTNF-α	DQ923808	5′- CGC*GGATCC* GTCAAATCATCTTC -3′	229-242	472bp
		5′- ACGC*GTCGAC* TCACAGGGCAATGATTCC -3′	685-700	
cIL-6	AF275796.1	5′- CGC*GGATCC* ATGAACTCCCTCTCCA -3′	1-16	624bp
		5′- ACGC*GTCGAC* TCACATTATCCGAACA -3′	609-624	

＊Restriction sites are indicated in italics

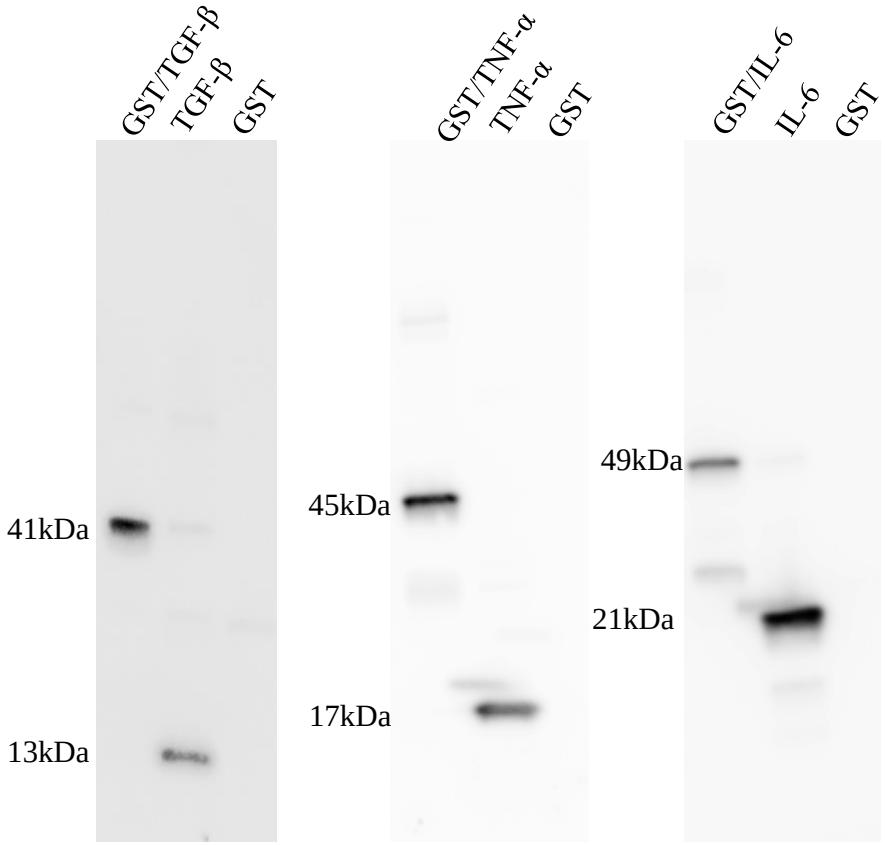

Fig. 2.1 Purification of recombinant cTGF-β, cTNF-α, and cIL-6.

Recombinant cTGF-β, cTNF-α, and cIL-6 were expressed by *E. coli* (BL21) and purified by using Glutathione-Sepharose 4 beads and Pre Scission protease. Recombinant proteins were detected by anti-TGF-β_1 antibody, anti-TNF-α antibody, and anti-IL-6 antibody. The molecular weights of cTGF-β, cTNF-α, cIL-6, and glutathione S transferase (GST) were 13 kDa, 17 kDa, 21 kDa, and 28 kDa, respectively.

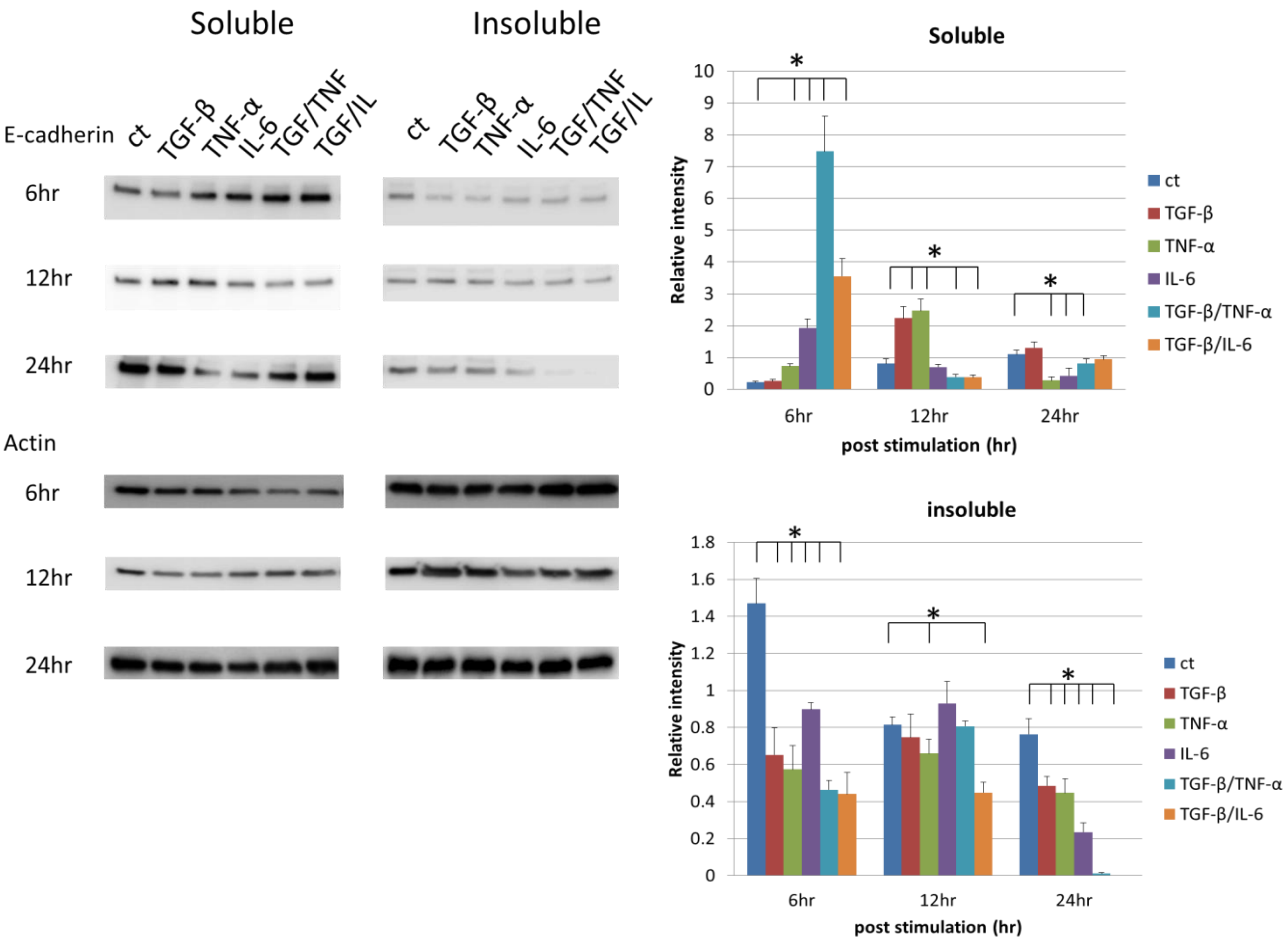

Fig.2.2 Reduction and shift of E-cadherin.

MDCK cells were stimulated with TGF-β (10 ng/mL), TNF-α (10 ng/mL), and/or IL-6 (10 ng/mL). After 6 hr, 12 hr, and 24 hr post-stimulation, cells were lysed with Triton X-100 buffer or SDS buffer. Expressions of E-cadherin were determined by western blot analysis. After 6 hr post-stimulation, localization of E-cadherin shifted from insoluble fraction to soluble fraction. After 24 hr post-stimulation, E-cadherin in insoluble fraction was significantly reduced.

＊: $p < 0.05$. Vertical bar represents SE.

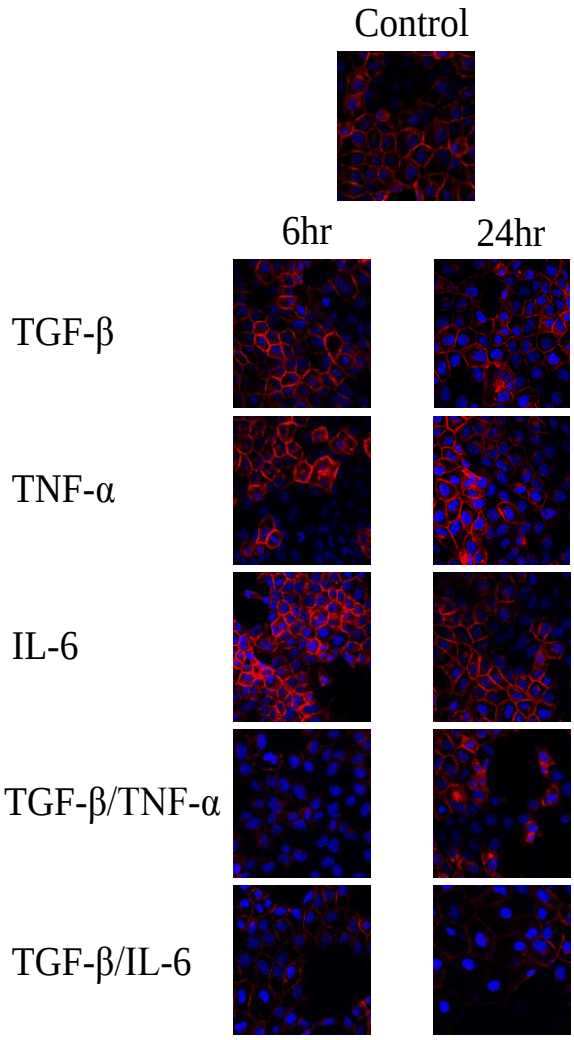

Fig.2.3 Change in the amount of cell surface E-cadherin.

MDCK cells were stimulated with TGF-β (10 ng/mL), TNF-α (10 ng/ml) and/or IL-6 (10 ng/mL). Six hours and 24 h post-stimulation, cells were fixed and immunostained with mouse anti-E-cadherin antibody, followed by Alexa 568-conjugated goat anti-mouse IgG. Nuclei were stained with DAPI. E-cadherin expression was reduced at the cell surface, especially in co-stimulating cells. Red: E-cadherin. Blue: DAPI.

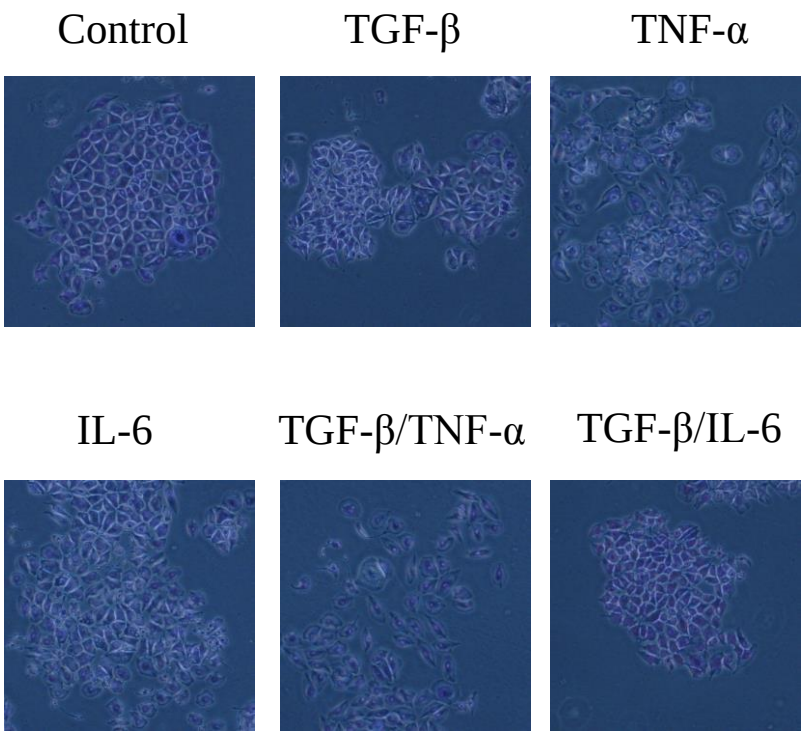

Fig.2.4 Morphological changes in MDCK cells.

MDCK cells were stimulated with TGF-β (10 ng/mL), TNF-α (10 ng/mL), and/or IL-6 (10 ng/mL). Six days post-stimulation, cells were fixed and stained with Wright-Giemsa stain. TGF-β and IL-6 did not substantially change the cell morphology. However, TNF-α and TGF-β/TNF-α weakened cell-cell adhesion interactions and induced morphological changes from cobble to spindle forms.

Chapter 3

Effects of inflammatory cytokines on EMT marker expressions in cMGT cells

3.1. Introduction

The epithelial–mesenchymal transition (EMT) is a complex biological process by which the morphology of polarized epithelial cells is converted to fibroblastic mesenchymal cells. EMT in cancer cell has been reported to be induced by various cytokines and related to tumor malignancy. For instance, human TGF-β was reported to induce EMT in human breast cancer cell (Li et al., 2014) and ovarian cancer cells (Gao et al., 2014).In addition, human TNF-α, human IL-6 and human IL-8 were also reported to induce EMT in various cancer cells (Fernando et al., 2011; Ho et al., 2012; Rokavec et al., 2014; Wang et al., 2013b). On the other hand, it has been well known that inflammation in microenvironment affects the growth of tumor (Coussens et al., 2013). As one of the distinguish feature of cIMC is severe inflammation associated with tumor mass, it is suspected that the inflammation has close relationship with the malignancy of cIMC. Actually, amount of infiltrations of tumor associate macrophage and secretions of TNF-α, IL-8 and IL-10 in hIBC patients were higher than in non-hIBC patients (Mohamed et al., 2014). These inflammatory cytokines were also reported to promote morphological change, cell migration and invasion in hIBC cell lines (Mohamed et al., 2014). Because clinical features of cIMC are similar to those of hIBC, it was hypothesized that inflammatory stimulation by various cytokines in the tumor microenvironment contributed the malignancy of cIMC through induction of EMT.

The purpose of this chapter was to investigate whether canine TGF-β, TNF-α and IL-6, which were successfully obtained in the previous chapter, induced EMT in cMGT cell lines by the evaluation of EMT marker expressions. In section 1, to evaluate the effects of inflammatory cytokines on cMGT cell, six cMGT cell lines were stimulated with cytokines and investigated whether the expression changes of EMT markers were induced by inflammatory stimulation. For further investigation, cMGT cell line was cloned and a clonal cell line was stimulated with cytokines to investigate effects of inflammatory stimulation in section 2.

Section 1: Expression changes of EMT markers in cMGT cell lines stimulated with cTGF-β, cTNF-α and cIL-6

3.1.2 Materials and methods

3.1.2.1 Cell culture

Canine MGT cell lines, CHMp, CHMm, CTBp, CTBm, CIPp and CIPm cell (Uyama et al., 2006) were used in this section (Table 3.1.1). Cells were cultured in RPMI1640 containing 10% FBS at a humidified atmosphere of 5% CO_2 and 37°C.

3.1.2.2 Reagent

Canine recombinant proteins, cTGF-β, cTNF-α and cIL-6, prepared as described in chapter 2 were used.

3.1.2.3 Cell stimulation

Six cMGT cell lines were stimulated with recombinant cTGF-β, cTNF-α and cIL-6 singly or coincidentally at a final concentration of 10 ng/mL. Stimulated cells were harvested at 24 hours post simulation.

3.1.2.4 Immunoblot analysis

Cell lysates were collected as described in chapter 2. Lysates of insoluble fraction of stimulated cells were used in a mixture of sample buffer (100 mM Tris-HCl, pH6.8, 2% sodium dodecyl sulfate (SDS), 12% 2-mercaptoethanol, 20% glycerol, and bromophenol blue). Samples were containing 10 μg of total protein per lane, and run on 4–15% Mini-PROTEAN TGX gel (Bio-Rad), then transferred to polyvinylidene fluoride (PVDF) membranes (Bio-Rad). The membranes were then incubated with mouse anti-E-cadherin antibody (1:2,000; BD Biosciences), rabbit anti-ZO-1 (1:2,000; Santa Cruz Biotechnology), mouse anti-vimentin (1:2,000; Millipore), mouse anti-N-cadherin (1:2,000; Abcam), rabbit anti-fibronectin (1:5,000; Dako Japan) and mouse anti-actin antibody (1:10,000; Millipore), followed by incubation with anti-mouse IgG conjugated to horseradish peroxidase (HRP) (1:10,000; GE Healthcare) and anti-rabbit IgG conjugated to HRP (1:10,000; GE Healthcare). Signals were detected using the Luminata Forte Western HRP substrate (Millipore). Quantifications of signals were performed by using ImageJ software.

3.1.3 Results

EMT marker expression patterns of non-stimulated cell were similar within CIP pair and not within CHM and CTB pairs. Difference expression patterns of EMT marker between CHMp and CHMm were E-cadherin, N-cadherin and ZO-1 (Fig. 3.1.1 and Fig. 3.1.2). Difference expression patterns of EMT marker between CTBp and CTBm were E-cadherin and N-cadherin (Fig. 3.1.3 and Fig. 3.1.4).Similar expression patterns of EMT marker between CIPp and CIPm were E-cadherin, N-cadherin, fibronectin and vimentin (Fig. 3.1.5 and Fig. 3.1.6).

Six cell lines of cMGT were stimulated with cTGF-β, cTNF-α and cIL-6. Expression changes of EMT markers were varied among these cell lines. In CHMp cells, expressions of ZO-1 were down-regulated by cTNF-α and cTGF-β/cIL-6 stimulations, and up-regulated by cIL-6 and cTGF-β/cTNF-α stimulations. Expressions of N-cadherin were up-regulated by cTGF-β, cTNF-α and cIL-6 stimulations. Expressions of fibronectin were down-regulated by all stimulations. Expressions of vimentin were down-regulated by all stimulations except cTGF-β stimulation. (Fig. 3.1.1). In CHMm cells, expressions of E-cadherin were up-regulated by cTNF-α and cIL-6 stimulations. Expressions of ZO-1 were down-regulated by cTGF-β, cIL-6 and cTGF-β/cTNF-α stimulations, and up-regulated by cTNF-α stimulation. Expressions of fibronectin were down-regulated by cTNF-α, cIL-6 and cTGF-β/cIL-6. Expressions of vimentin were down-regulated by all stimulations (Fig. 3.1.2). In CTBp cells, expressions of E-cadherin

were down-regulated by all stimulations except cTGF-β stimulation. Expressions of ZO-1 were up-regulated by all stimulations except cTGF-β/cTNF-α stimulation. Expressions of fibronectin were up-regulated by all stimulations except cTGF-β stimulation. Expressions of vimentin were down-regulated by all stimulations (Fig. 3.1.3). In CTBm cells, expressions of E-cadherin were down-regulated by all stimulations except cTGF-β stimulation, and up-regulated by cTGF-β stimulation. Expressions of ZO-1 were down-regulated by all stimulations except cTGF-β stimulation. Expressions of fibronectin were up-regulated by cTGF-β and cTGF-β/cIL-6 stimulations, and down-regulated by cTNF-α, cIL-6 and cTGF-β/cTNF-α stimulations. Expressions of vimentin were down-regulated by cTNF-α, cIL-6 and cTGF-β/cTNF-α stimulations (Fig. 3.1.4). In CIPp cells, expressions of E-cadherin were down-regulated by all stimulations except cTGF-β stimulation. Expressions of ZO-1 were up-regulated by cTGF-β/cTNF-α stimulation. Expressions of N-cadherin were down-regulated by cTNF-α stimulation. Expressions of vimentin were up-regulated by cTGF-β/cIL-6 stimulation (Fig. 3.1.5). In CIPm cells, expressions of E-cadherin were down-regulated by cTGF-β, cTNF-α and cTGF-β/cTNF-α stimulations, and up-regulated by cTGF-β/cIL-6 stimulation. Expressions of ZO-1 were up-regulated by all stimulations. Expressions of N-cadherin were up-regulated by cTGF-β/cTNF-α stimulation, and down-regulated by cIL-6 stimulation. Expressions of fibronectin were up-regulated by cIL-6 and cTGF-β/cTNF-α stimulations, and down-regulated

by cTNF-α and cTGF-β/cIL-6 stimulations. Expressions of vimentin were up-regulated by cTGF-β/cTNF-α and cTGF-β/cIL-6 stimulations (Fig. 3.1.6).

3.1.4 Discussion

In this section, it was investigated whether stimulation with single and combination of canine recombinant cytokine TGF-β, TNF-α and IL-6 induced EMT in cMGT cell lines. Although IL-6 was reported to induce the decrease in E-cadherin in breast cancer cell lines (Sullivan et al., 2009), it was also reported not to show the reaction in other breast cancer cell lines (Asgeirsson et al., 1998). These results indicate that the reactivity to cytokine stimulations may be different in each cell line. Considering the difference in reactivity of individual cells, six cMGT cell lines which derived from primary and metastatic lesions of 3 cases were subjected to this study.

In CHMp cells, cTGF-β induced EMT change in N-cadherin, and MET change, reverse phenomenon of EMT, in fibronectin. Canine TNF-α induced EMT change in ZO-1 and N-cadherin, and MET change in fibronectin and vimentin. Canine IL-6 induced EMT change in N-cadherin, and MET change in ZO-1, fibronectin and vimentin. Canine TGF-β/cTNF-α induced MET change in ZO-1, fibronectin and vimentin. Canine TGF-β/cIL-6 induced EMT change in ZO-1, and MET change in fibronectin and vimentin. In CHMm cells, cTGF-β induced EMT change in ZO-1, and MET change in vimentin. Canine TNF-α induced MET change in E-cadherin, ZO-1, fibronectin and vimentin. Canine IL-6 induced EMT change in ZO-1, and MET change in E-cadherin, fibronectin and vimentin. Canine TGF-β/cTNF-α induced EMT

change in ZO-1, and MET change in vimentin. Canine TGF-β/cIL-6 induced MET change in fibronectin and vimentin. In CTBp cells, cTGF-β induced MET change in ZO-1 and vimentin. Both cTNF-α and cIL-6 induced EMT change in E-cadherin and fibronectin, and MET change in ZO-1 and vimentin. Canine TGF-β/cTNF-α induced EMT change in E-cadherin and fibronectin, and MET change in vimentin. Canine TGF-β/cIL-6 induced EMT change in E-cadherin and fibronectin, and MET change in ZO-1 and vimentin. In CTBm cells, cTGF-β induced EMT change in fibronectin, and MET change in E-cadherin. Canine TNF-α, cIL-6 and cTGF-β/cTNF-α induced EMT change in E-cadherin and ZO-1, and MET change in fibronectin and vimentin. Canine TGF-β/cIL-6 induced EMT change in E-cadherin, ZO-1 and fibronectin. In CIPp cells, cTNF-α induced EMT change in E-cadherin, and MET change in N-cadherin. Canine IL-6 induced EMT change in E-cadherin. Canine TGF-β/cTNF-α induced EMT change in E-cadherin, and MET change in ZO-1. Canine TGF-β/cIL-6 induced EMT change in E-cadherin and vimentin. In CIPm cells, cTGF-β induced EMT change in E-cadherin, and MET change in ZO-1. Canine TNF-α induced EMT change in E-cadherin, and MET change in ZO-1 and fibronectin. Canine IL-6 induced EMT change in fibronectin, and MET change in ZO-1 and N-cadherin. Canine TGF-β/cTNF-α induced EMT change in E-cadherin, N-cadherin, fibronectin and vimentin, and MET change in ZO-1. Canine TGF-β/cIL-6 induced EMT change in vimentin, and MET change in E-cadherin, ZO-1 and fibronectin. Although cell lines from the same dog

showed similar tendency of expression change of EMT markers, effects of cytokines on cMGT cell lines were not always constant. As cMGT cell lines used in this study were derived from tumor tissues of spontaneous MGT cases and had not been monocloned, these cell lines were thought to have heterogeneous cell populations. It was assumed that the accumulation of different reactivities of each cell population to cytokine stimuli made the reactivity of each cell line diverse. Thus, monoclonal cell line was thought to be suitable for investigation of the effects of cytokines.

CIPp cell line was estimated to be sensitive to the stimulations comparing to other cell lines, because loss or reduce of E-cadherin were induced by cTNF-α, cIL-6, cTGF-β/cTNF-α and cTGF-β/cIL-6 stimulations, and acquisition of vimentin were induced by cTGF-β/cIL-6 stimulation. Therefore, cloning of CIPp cells and evaluation of cell features based on the EMT marker expression were conducted to perform in section 2.

Table3.1.1 Characters of cMGT cell lines.

Cell line	Breed	Age(years)	Diagnosis	Clinical stage	TNM	Origin of tumor
CHMp	Mongrel	12	Inflammatory adenocarcinoma	Ⅳ	T4N1M1	Primary mass
CHMm						Metastatic LN[1]
CTBp	Mongrel	12	Inflammatory adenocarcinoma	Ⅳ	T4N1M0	Primary mass
CTBm						Metastatic LN[1]
CIPp	Shih Tzu	10	Adenocarcinoma	Ⅳ	T1cN1M1	Primary mass
CIPm						Pleural effusion

[1]LN, lymph node

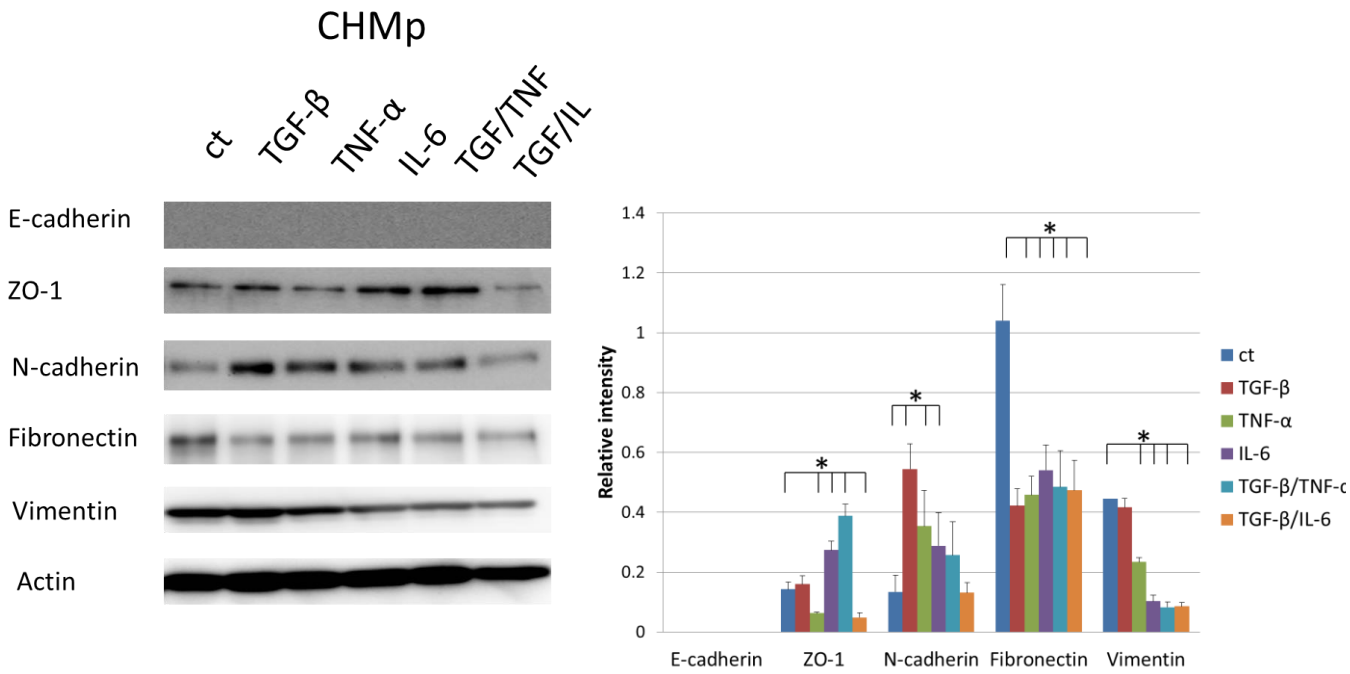

Fig. 3.1.1 Western blot of stimulated CHMp cells in insoluble fractions.

Cells were stimulated with cTGF-β, cTNF-α and cIL-6 at a final concentration of 10 ng/ml. Expressions of ZO-1 were reduced by cTNF-α and cTGF-β/cIL-6 stimulations and increased by cIL-6 and cTGF-β/cTNF-α stimulations. Expressions of N-cadherin were increased by cTGF-β, cTNF-α and cIL-6 stimulations. Expressions of fibronectin were reduced by all stimulations. Expressions of vimentin were reduced by all stimulations except cTGF-β stimulation.

＊: $p < 0.05$. Vertical bar represents SE.

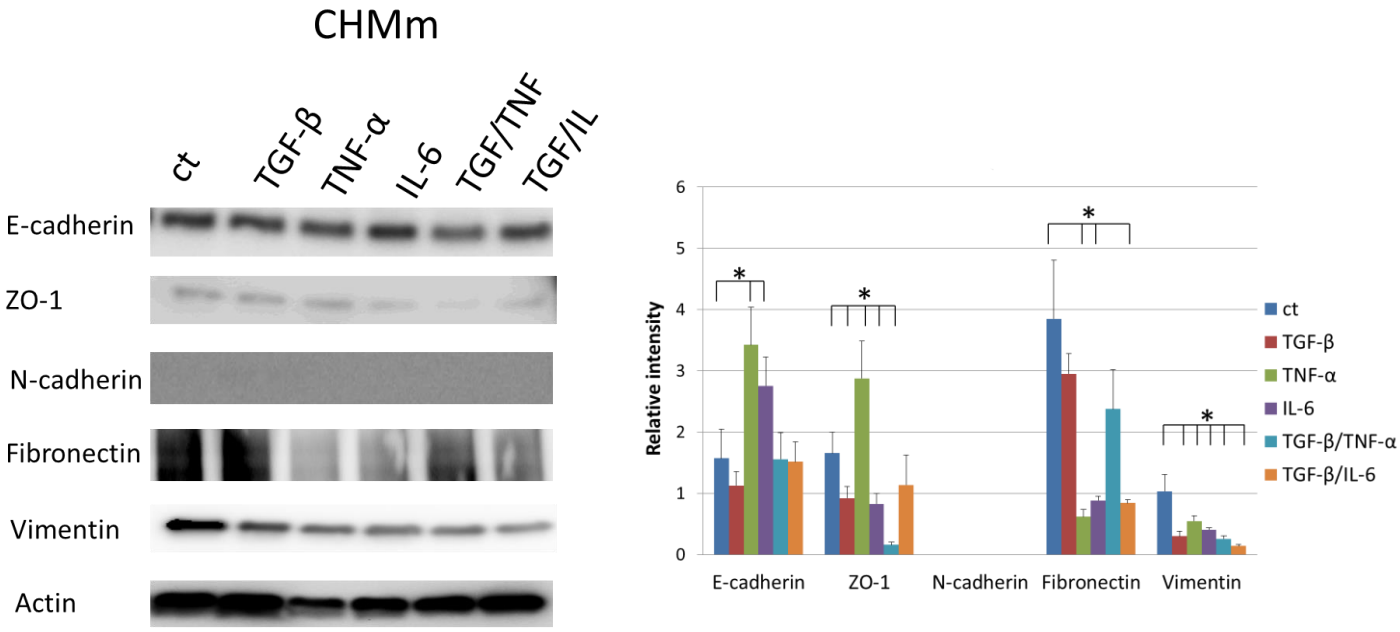

Fig. 3.1.2 Western blot of stimulated CHMm cells in insoluble fractions.

Cells were stimulated with cTGF-β, cTNF-α and cIL-6 at a final concentration of 10 ng/ml. Expressions of E-cadherin were increased by cTNF-α and cIL-6 stimulations. Expressions of ZO-1 were reduced by cTGF-β, cIL-6 and cTGF-β/cTNF-α stimulations and increased by cTNF-α stimulation. Expressions of fibronectin were reduced by cTNF-α, cIL-6 and cTGF-β/cIL-6. Expressions of vimentin were reduced by all stimulations.

＊: $p < 0.05$. Vertical bar represents SE.

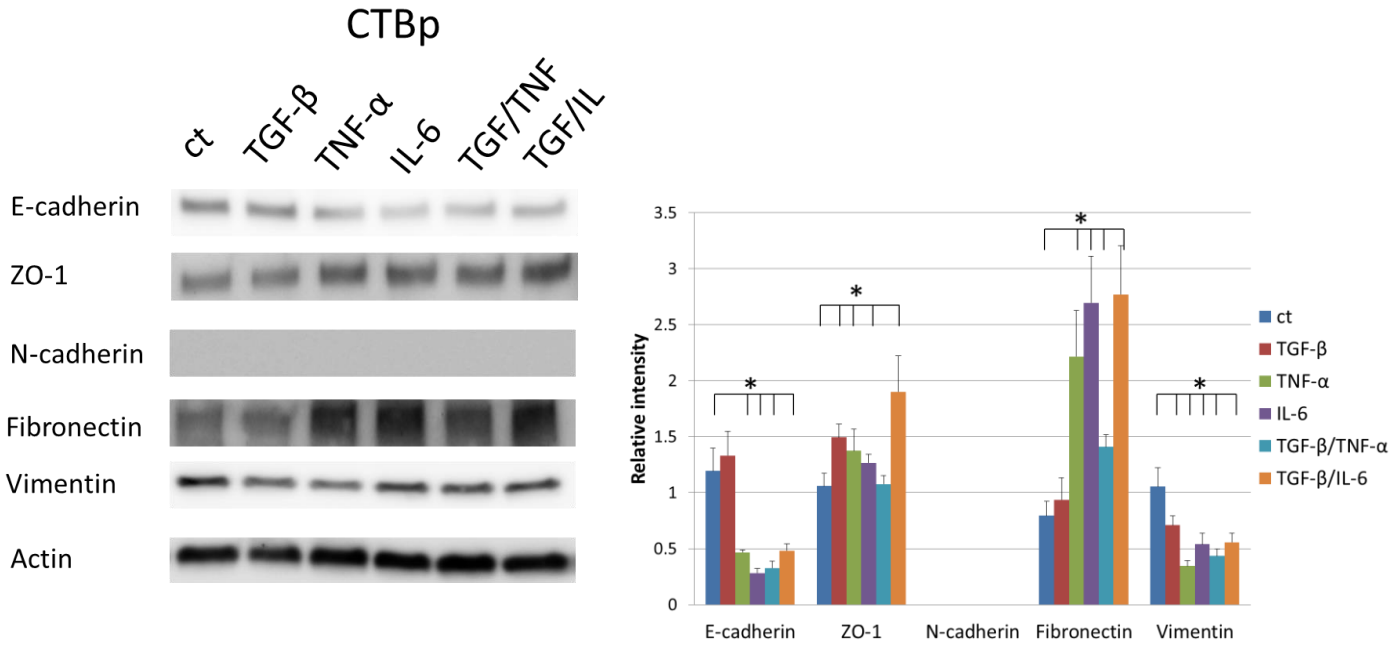

Fig. 3.1.3 Western blot of stimulated CTBp cells in insoluble fractions.

Cells were stimulated with cTGF-β, cTNF-α and cIL-6 at a final concentration of 10 ng/ml. Expressions of E-cadherin were reduced by all stimulations except cTGF-β stimulation. Expressions of ZO-1 were increased by all stimulations except cTGF-β/cTNF-α stimulation. Expressions of fibronectin were increased by all stimulations except cTGF-β stimulation. Expressions of vimentin were reduced by all stimulations.

＊: $p < 0.05$. Vertical bar represents SE.

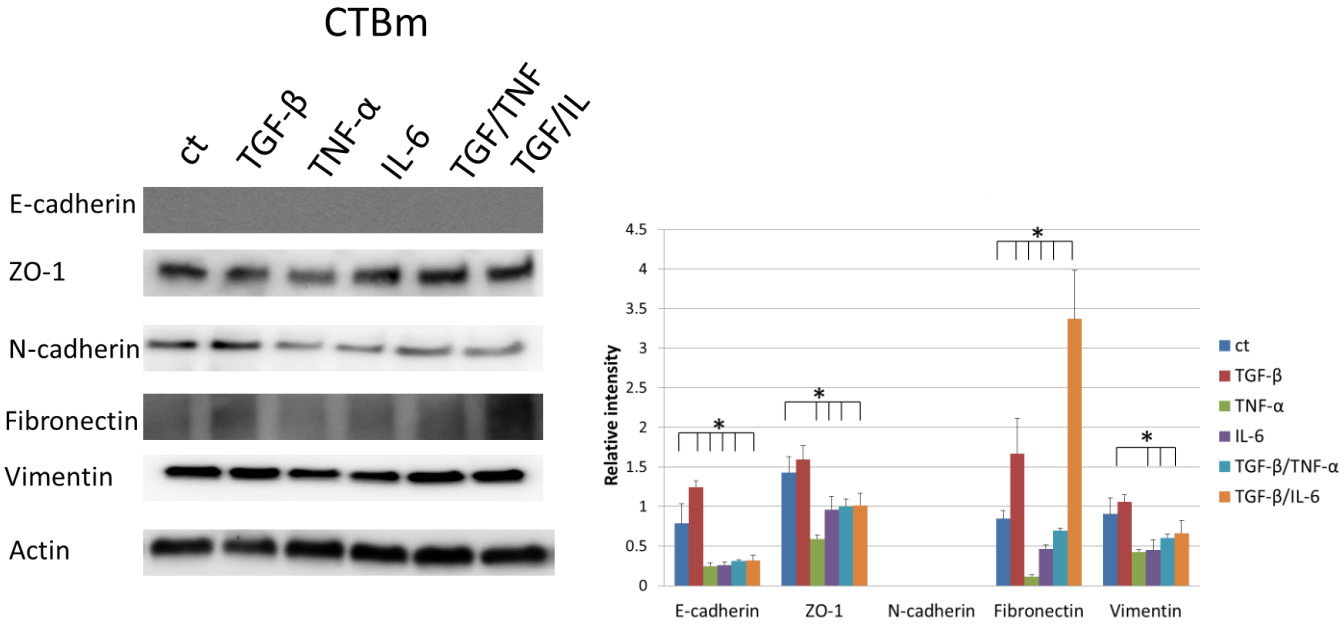

Fig. 3.1.4 Western blot of stimulated CTBm cells in insoluble fractions.

Cells were stimulated with cTGF-β, cTNF-α and cIL-6 at a final concentration of 10 ng/ml. Expressions of E-cadherin were reduced by all stimulations except cTGF-β stimulation and increased by cTGF-β stimulation. Expressions of ZO-1 were reduced by all stimulations except cTGF-β stimulation. Expressions of fibronectin were increased by cTGF-β and cTGF-β/cIL-6 stimulations and reduced by cTNF-α, cIL-6 and cTGF-β/cTNF-α stimulations. Expressions of vimentin were reduced by cTNF-α, cIL-6 and cTGF-β/cTNF-α stimulations.

＊: $p < 0.05$. Vertical bar represents SE.

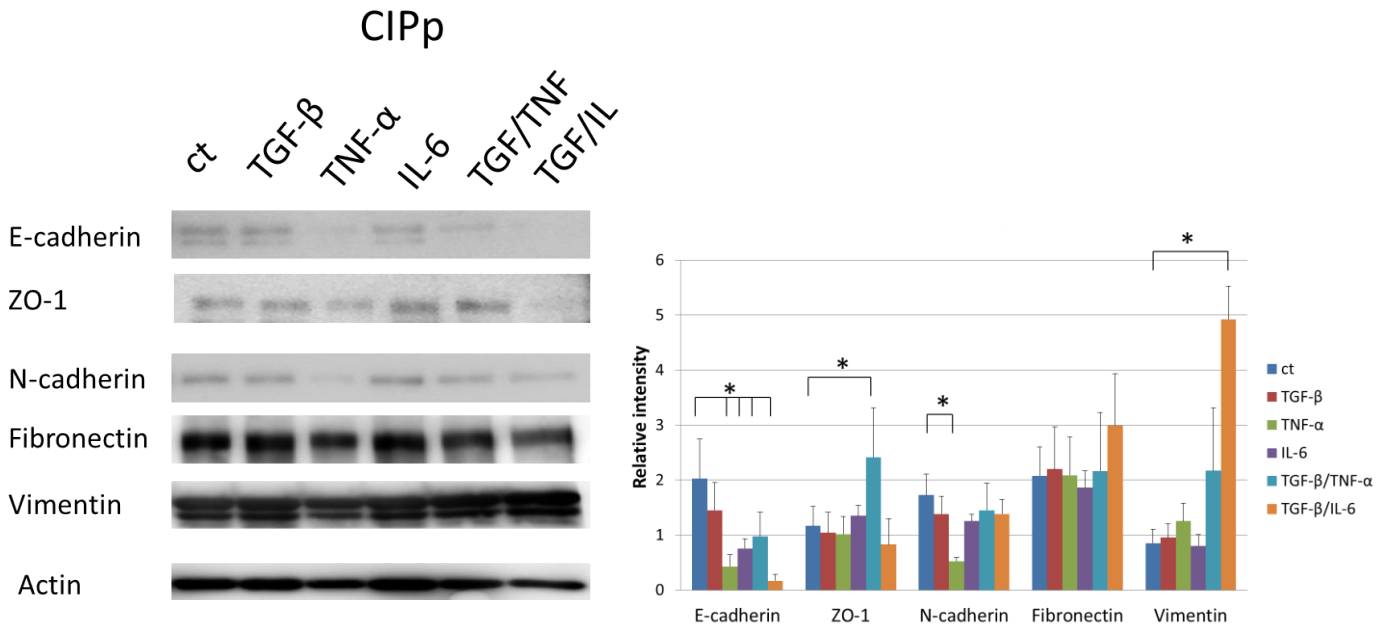

Fig. 3.1.5 Western blot of stimulated CIPp cells in insoluble fractions.

Cells were stimulated with cTGF-β, cTNF-α and cIL-6 at a final concentration of 10 ng/ml. Expressions of E-cadherin were reduced by all stimulations except cTGF-β stimulation. Expressions of ZO-1 were increased by cTGF-β/cTNF-α stimulation. Expressions of N-cadherin were reduced by cTNF-α stimulation. Expressions of vimentin were increased by cTGF-β/cIL-6 stimulation.

＊: $p < 0.05$. Vertical bar represents SE.

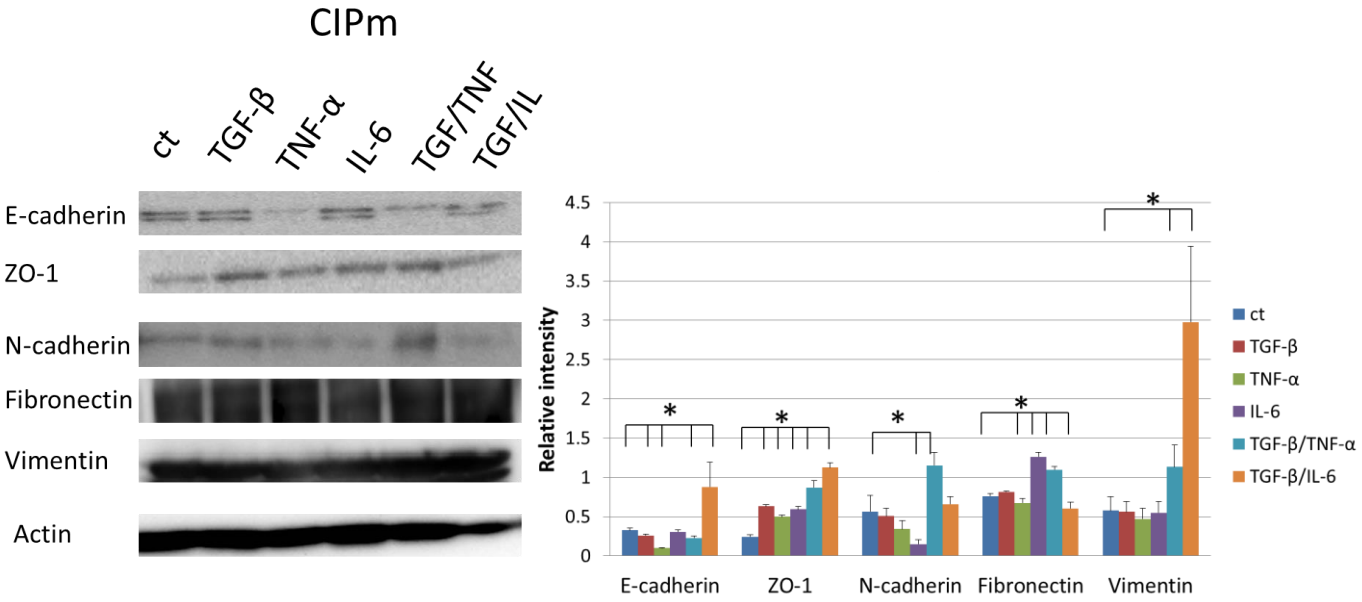

Fig. 3.1.6 Western blot of stimulated CIPm cells in insoluble fractions.

Cells were stimulated with cTGF-β, cTNF-α and cIL-6 at a final concentration of 10 ng/ml. Expressions of E-cadherin were reduced by cTGF-β, cTNF-α and cTGF-β/cTNF-α stimulations, and increased by cTGF-β/cIL-6 stimulation. Expressions of ZO-1 were increased by all stimulations. Expressions of N-cadherin were increased by cTGF-β/cTNF-α stimulation, and reduced by cIL-6 stimulation. Expressions of fibronectin were increased by cIL-6 and cTGF-β/cTNF-α stimulations, and reduced by cTNF-α and cTGF-β/cIL-6 stimulations. Expressions of vimentin were increased by cTGF-β/cTNF-α and cTGF-β/cIL-6 stimulations.

＊: $p < 0.05$. Vertical bar represents SE.

Section 2: Expression changes of EMT markers in cloned CIPp-4b cell line stimulated with cTGF-β, cTNF-α and cIL-6

3.2.2 Materials and methods

3.2.2.1 Cells

CIPp cell line was cultured in RPMI1640 containing 10% FBS. Cells were maintained in a humidified atmosphere of 5% CO_2 at 37°C.

3.2.2.2 Cloning of CIPp cell

CIPp cells were cloned by limiting dilution method. An average of 0.5 cells per well were plated onto 96 well plates in RPMI1640 containing 20% FBS. After confirmations of forming single colony, cloned cells were properly passaged to large scales. Immunoblot analysis was performed to examine the characteristics of cloned CIPp cell lines. Cells were lysed with RIPA buffer (50mM Tris–HCl pH 7.5, 150mM NaCl, 5mM EDTA, 1% Triton X-100, 0.1% SDS, protease inhibitor cocktail tablets (Roche, NJ, USA), 10mM NaF, 2mM Na_3VO_4). Whole cell lysates were mixed with sample buffer and run on SDS-PAGE gel containing 10% acrylamide, then blotted to PVDF membrane. The membranes were incubated with anti-E-cadherin antibody (1:2,000), rabbit anti-ZO-1 (1:2,000), mouse anti-vimentin (1:2,000), mouse anti-N-cadherin (1:2,000), rabbit anti-fibronectin (1:5,000) and mouse anti-actin antibody (1:10,000), followed

by incubation with anti-mouse IgG conjugated to HRP (1:10,000) and anti-rabbit IgG conjugated to HRP (1:10,000, GE Healthcare). Signals were detected using the Luminata Forte Western HRP substrate (Millipore).

3.2.2.3 Cell stimulation

Among monoclonal cells derived from CIPp cell line, cell line which showed epithelial phenotype was selected for cell stimulation with inflammatory cytokines. Clonal cell was stimulated as described in section 1.

3.2.2.4 Immunoblot analysis

Protein collection and western blot analysis of stimulated clonal cell line was performed as described in section 1.

3.2.3 Results

3.2.3.1 Cloning of CIPp cell

Eleven single colonies were obtained, and cultured over 20 passages. Cloned cell lines were renamed as CIPp-1b, -1d, -2a, -3c, -3d, -4b, -4c, -4d, -5c, -6d and -7d, respectively. Cell shape was round to spindle, and most of them showed spindle shape (Fig. 3.2.1). Expressions of EMT markers were shown in Fig. 3.2.2. Most of cloned cell lines exhibited the features of mesenchymal cells, such as low expressions of E-cadherin and high expressions of vimentin and fibronectin. On the contrary, CIPp-4b showed higher expression E-cadherin and lower expression of fibronectin among cloned cell lines. Therefore, CIPp-4b cells were used for the stimulation by cTGF-β, cTNF-α and cIL-6.

3.2.3.2 Changes in EMT marker expressions in CIPp-4b cells

Changes of EMT markers expressions in stimulated CIPp-4b were evaluated by western blot analysis. Expressions of E-cadherin and ZO-1 were down-regulated by all stimulations. Expressions of N-cadherin were up-regulated by cTGF-β, cTNF-α, cIL-6 and cTGF-β/cTNF-α stimulations. Expressions of fibronectin were up-regulated by all stimulations. Expressions of vimentin were up-regulated by cIL-6, cTGF-β/cTNF-α and cTGF-β/cIL-6 stimulations.

3.2.4 Discussion

Cancer tissue contains several types of cells with heterogeneity in their phenotypes (Kan et al., 2010). Among them, malignant types of cells metastasized to distant organs via EMT (Tsuji et al., 2009). EMT is thought to strongly relate to tumor malignancy. Although investigation of relationship between inflammatory stimulation and EMT was performed in the previous section, effects of inflammatory stimulation were unclear. This was thought to be due tumor heterogeneity. Therefore, cloning of CIPp cells and investigation of EMT marker change of clonal cells stimulated with cTGF-β, cTNF-α and cIL-6 were performed in this section. For the observation of clearly EMT marker changes, CIPp-4b cells which showed the most epithelial phenotype among cloned CIPp cells were selected to investigate transition from epithelial to mesenchymal phenotype by stimulations of recombinant cytokines in this section. After stimulation with cytokines, CIPp-4b cells showed EMT with tipical expression of several EMT markers in comparison to parental CIP cells in the previous section.

All stimulations reduced the expression of E-cadherin and ZO-1, while increased the expressions of fibronectin. Canine TGF-β, cTNF-α, cIL-6 and cTGF-β/cTNF-α stimulations increased the expressions of N-cadherin, and cIL-6, cTGF-β/cTNF-α and cTGF-β/cIL-6 stimulations increased the expressions of vimentin. CIPp-4b cells were suggested to be sensitive to stimulations of these cytokines and be caused partial EMT by these cytokines. These marker

changes were suggested to be related to tumor cell abilities of invasion and migration. Down-regulation of E-cadherin and up-regulations N-cadherin and fibronectin reported to promote invasion and migration in colorectal cancer cells (Wang et al., 2013b). Up-regulation of N-cadherin was reported to promoted cancer cell migration (Gao et al., 2014). Based on these results and literatures, CIPp-4b cell line was thought to be suitable to investigate the relationship between EMT induced by inflammatory cytokines and the malignant progression of cMGT.

Cytokines purified in chapter 2 induced EMT in CIPp-4b cells *in vitro*, though changes of cell properties did not completely match the features of EMT. There was a limitation that evaluations of tumor growth, distant metastasis and lymph node metastasis were not able to performe in this *in vitro* study. To investigate whether these EMT changes induced by growth factor and inflammatory cytokines reproduced the malignancy of cIMC including rapid tumor growth, distant metastasis and lymph node metastasis, *in vivo* study was needed. In next chapter, CIPp-4b cells were transplanted into mice and stimulated by cytokines.

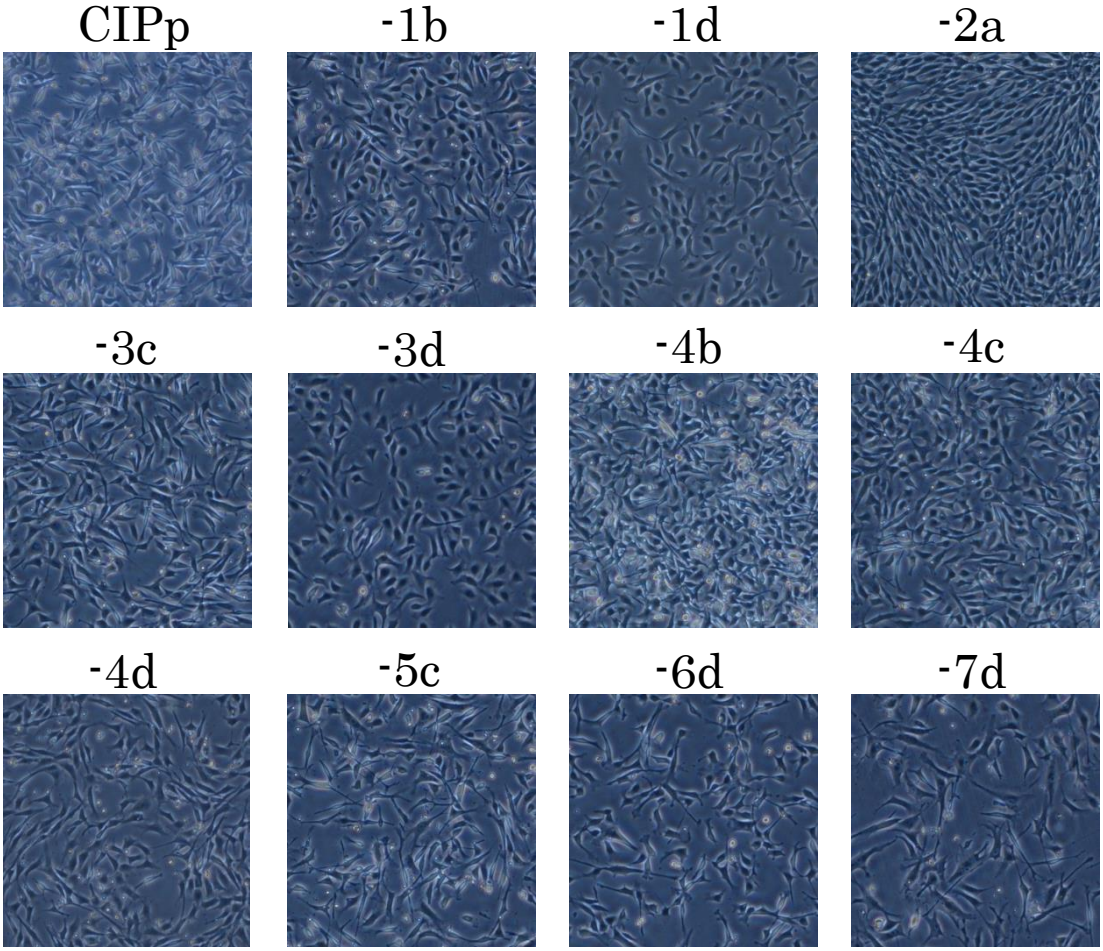

Fig. 3.2.1 Morphologies of CIPp cell line and cloned CIPp cell lines.

CIPp cell line was cloned by limited dilution methods. Eleven cell lines were cloned. Cell morphologies were from epithelial-like to fibroblastic.

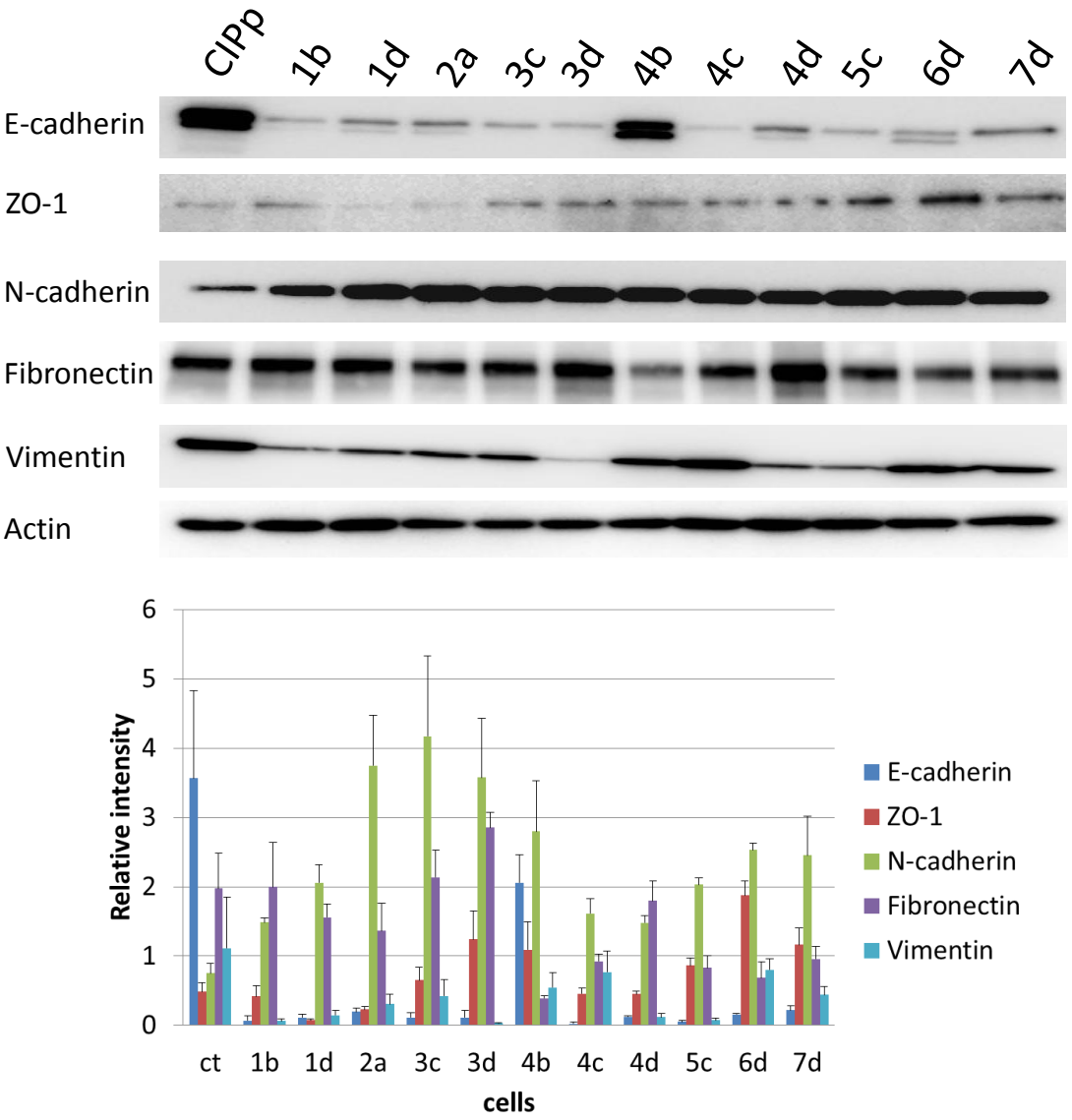

Fig. 3.2.2 Expressions of EMT markers in 11 cloned CIPp cell lines.

CIPp cell contained various types of cells. CIPp-4b cell showed high expression of E-cadherin, expression of ZO-1 and low expression of fibronectin among them.

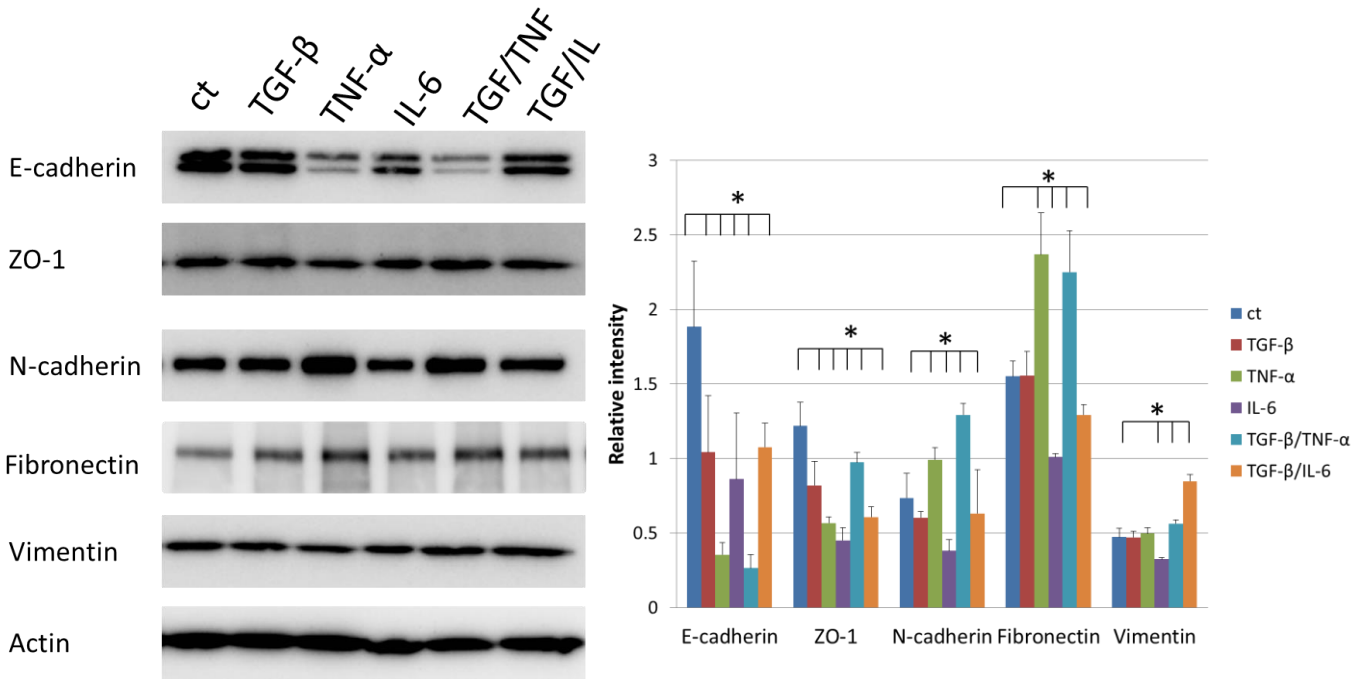

Fig. 3.2.2 Changes of EMT markers in CIPp-4b cell.

CIPp-4b cell was stimulated with cTGF-β, cTNF-α and cIL-6 at a final concentration of 10 ng/ml. Expressions of E-cadherin and ZO-1 were reduced by all stimulations. Expressions of N-cadherin were increased by cTGF-β, cTNF-α, cIL-6 and cTGF-β/cTNF-α stimulations. Expressions of fibronectin were increased by all stimulations. Expressions of vimentin were increased by cIL-6, cTGF-β/cTNF-α and cTGF-β/cIL-6 stimulations.

＊: $p < 0.05$. Vertical bar represents SE.

Chapter 4

Effects of inflammatory stimulations in the cMGT transplanted mouse model

4.1 Introduction

Inflammation is one of the important factors to progress tumor malignancies (Balkwill, 2006, 2009; Fuxe and Karlsson, 2012; Weitzenfeld et al., 2013). Various immune cells are activated in the tumor microenvironment and various factors including growth factors and inflammatory cytokines are secreted (Fuxe and Karlsson, 2012). These factors may work multiply rather independently to progress tumor malignancy (Balkwill and Mantovani, 2001; Mohamed et al., 2014).

It was reported that overexpression or silencing of EMT initiator genes, such as Snail and Twist, affected tumor malignancies (Kudo-Saito et al., 2009; Morel et al., 2012; Yang et al., 2004). Several *in vitro* studies indicated that EMT initiator genes were activated by EMT inducing factors, such as growth factors and inflammatory cytokines (Brown et al., 2004; Fernando et al., 2011; Fuxe and Karlsson, 2012; Kamitani et al., 2011; Li et al., 2012; Miettinen et al., 1994; Nicolás et al., 2003). In transplanted model of human breast cancer cells, progression of EMT was observed in the formed tumor and circulating tumor cells (Bonnomet et al., 2012). However, *in vivo* analysis of the role and significance of EMT inducing factors for tumor malignancy was limited. In addition, no *in vivo* investigation for the relationship between tumor progression or malignancy of cIMC and EMT which induced by these cytokines was performed in veterinary medicine.

In the previous chapter, inflammatory stimulations with cytokines and their combination induced EMT changes in cMGT cell lines. However, effects of inflammatory stimulation on tumor mass were not surveyed. Transplanted mouse models were thought to be helpful to investigate the relationship between these EMT changes and malignant progression of cMGT. Therefore, the purpose of this chapter was to investigate whether EMT changes induced by inflammatory cytokines initiate or accelerate tumor malignancy such as proliferation and distant and lymph node metastasis.

4.2 Materials and methods

4.2.1 Cells

CIPp-4b cell line was used for a transplanted mouse models. CIPp-4b cells were maintained in RPMI1640 containing 10% FBS. Cells were maintained in a humidified atmosphere of 5% CO_2 at 37°C.

4.2.2 Reagent

Canine recombinant proteins, cTGF-β, cTNF-α and cIL-6, were expressed and purified as described in chapter 2 were used.

4.2.3 Animals

Thirty six five-week-old female BALB/c nude mice (Japan SLC, Shizuoka, Japan) were used for CIPp-4b cell xenografted mouse model. The experiment was approved by the Animal Care Committee of the Graduate School of Agricultural and Lifesciences, the University of Tokyo.

4.2.4 Transplantation and local stimulations

Three days before transplantation, the mice were irradiated with X-ray at a dose of 4

Gray. For transplantation, 5 x 10^5 CIPp-4b cells were suspended in 100 μL of PBS. Cells were subcutaneously injected into their left axilla. After transplantation, tumor size, body weight and food consumption were measured 3 times a week. The volume of tumor was calculated the following formula:

$$\text{Tumor volume } (mm^3) = (\text{length} \times \text{width}^2) / 2$$

When tumor width exceeded 5mm, stimulations started, and stimulations at seven days interval were performed once a week. Fifty ng of cTGF-β, cTNF-α, cIL-6, cTGF-β/cTNF-α and cTGF-β/cIL-6 was locally injected around formed tumor based on the results of chapter 3. PBS was used for control and diluents. Endpoints of this study were determined as tumor growth to cover their arm, or severe clinical signs. After sacrifice, tumor, lung and inguinal lymph node were collected. Collected samples were fixed in 10% neutral buffered formalin and embedded in paraffin. Sections of 4 μm were stained with hematoxylin-eosin stain.

4.2.5 Immunofluorescent double staining

The sections of tumor and metastasized lung and lymph node were evaluated by immunofluorescent staining. The sections were deparaffinized, and antigen epitope was retrieved by 10mM sodium citrate buffer, pH6.0 for 5min at 121°C. After epitope retrieval, nonspecific protein bindings were blocked using PBST containing 5% normal goat serum for

1hour at room temperature. Then sections were incubated with rabbit anti-E-cadherin antidody (1:300) and mouse anti-vimentin antibody (1:500) simultaneously at 4°C over-night. After incubation, sections were incubated with Fluorescein goat anti-rabbit IgG (H+L) (1:300) and Alexa Fluor 568 goat anti-mouse IgG (H+L) (1:300) simultaneously for 1 hour at room temperature with light interception. Then, slides were mounted in DAPI containing Vectashield mounting medium. Fluorescent images were scanned by LSM 700.

4.2.6 Statistical analysis

Statistical analyses of body weight of transplanted mice and growth of tumor were done using Student's t-test. Values of $p < 0.05$ were considered statistically significant.

4.3 Results

4.3.1 Mouse xenoglaft model

All of mice transplanted with CIPp-4b cells successfully formed tumor mass. During the experiment, body weight and food consumptions of mice showed no significant reduction (Fig.4.1). Severe clinical signs were not observed, but some tumor completely covered the left arm of the mouse at 14 days post stimulation. Therefore, the experiment was ended at 14 days. Tumors stimulated with cTGF-β significantly grew up in comparison to control at 14 days post stimulation (Fig.4.2). Stimulations with cTGF-β and cTGF-β/cTNF-α significantly increased the volumes of tumor in comparison to control group at 14 days post stimulation (Fig.4.2). Necrosis of the center of formed mass was observed in all mice (data not shown). Distinctive changes were not observed in intratumoral area with all stimulations comparing to control (data not shown). The metastatic lesions were observed in lymph node in one of 6 cTNF-α stimulated mice (Fig.4.5) and in lung in one of 6 cTGF-β/cIL-6 stimulated mice (Fig.4.6). Lymph node was completely replaced by tumor cells.

4.3.2 Immunofluorescent stain of primary and metastatic lesions

Primary tumors and metastatic lesions, lung and inguinal lymph node, were stained with E-cadherin and vimentin simultaneously. As the host of anti-vimentin antibody was mouse,

cells derived from transplanted cells were specifically stained in this study. In the primary tumor, expressions of vimentin were high and expressions of E-cadherin were low on the border especially in mice with cTGF-β/cTNF-α stimulation (Fig.4.3). In the center of tumors, areas of E-cadherin expressions and vimentin expressions were mixed, but merges of both EMT markers were scarcely observed and all stimulations did not make difference in EMT marker expressions (Fig.4.4). In the lymph node metastatic lesion, both E-cadherin and vimentin were expressed, but expressions of vimentin were dominant (Fig.4.5 (b)). In the lung metastatic lesions, tumor cells exhibited high expressions of vimentin (Fig.4.6 (b)). Expression patterns of E-cadherin and vimentin in metastatic foci were similar to these of medial tumor (Fig.4.4, Fig.4.5(b) and Fig.4.6 (b)).

4.4 Discussion

In this chapter, it was evaluated whether EMT changes induced by growth factor and inflammatory cytokines affected on tumor growth and metastasis to lymph node and distant organs in cMGT cell transplanted mice. Size of tumor stimulated with cTGF-β and cTGF-β/cTNF-α was significantly larger than that of control at 14 days post stimulation. In addition, one of six mice with cTNF-α stimulation formed lymph node metastasis and one of six mice with cTGF-β/cIL-6 stimulation formed lung metastasis, while no metastasis was observed in control group. Inflammation was known as one of exacerbating factors of cancer (Balkwill and Mantovani, 2001). It was reported that tumor volume was increased by TGF-β stimulation in lung cancer transplanted mouse model (Abulaiti et al., 2013). In that report, activation of Smad pathway by TGF-β stimulation was suggested to accelerate the tumor growth. Functions of TGF-β via Smad pathway were reported to be enhanced by co-stimulation with inflammatory cytokines such as TNF-α, IL-1β and IFN-γ in the same lung cancer cell line (Liu, 2008). Increase of tumor volume by cTGF-β and cTGF-β/cTNF-α stimulation might be due to activation of Smad pathway by TGF-β stimulation in this study.

Lymph node metastasis was induced by cTNF-α stimulation in one of six mice in this study. TNF-α stimulation was reported to induce lymph node metastasis in melanoma transplanted mouse model (Peppicelli et al., 2014). By the stimulation of TNF-α, the induction

of VEGF-C expression, which is a major lymphangiogenesis factor, was observed. Because injected cTNF-α stimulated not only tumor cells, but also tomor microenvironment in this study, various cytokines which supported lymph node metastasis might be released and cause lymph node metastasis. In addition, cTGF-β/cIL-6 stimulation induced lung metastasis in one of six mice. On the other hand, tumor volume with its stimulation was not significantly larger than that with no stimulation. It was reported that complex stimulation of cytokines and hormone induced increase of metastatic potential and reduction of tumor volume in comparison to unstimulated group in breast cancer cell transplanted model (Weitzenfeld et al., 2013). In this report, they discussed that increase of metastatic potential was due to the down-regulation of E-cadherin and up-regulation of CD44 and MMP9 which were induced by the stimulation. They also suggested that the enhancement of apoptosis induction might reduce the tumor volume. Although cytokines used for stimulation were not identical, the similar phenomena were thought to occur in this study.

Although tumor proliferation and metastasis were promoted by growth factor and cytokine stimulations, obvious morphological changes indicating EMT in tumor tissue were not observed in the histopathological evaluation of HE staining. To evaluate whether EMT was involved in tumor malignancy which was progressed by growth factor and inflammatory stimulations, expressions of E-cadherin and vimentin were investigated by immunofluorescent

double staining. In the formed tumor, larger numbers of cells which showed reduction of E-cadherin and high expression of vimentin were observed in the edge of tumor than in the center of tumor. On the other hand, cells in lymph node and distant metastasis lesion showed similar expression patterns to the center of tumor. It has been proposed that EMT occurred in invasive front of malignant tumor, and tumor cells which underwent EMT invaded into vascular system and metastasize to distant area, and then MET occurred in metastatic foci (Tsai and Yang, 2013). These findings were considered to support it. However, the most attenuation of E-cadherin expression was observed in cTGF-β/cTNF-α stimulated mice which did not form metastasis. As lymph node and distant metastasis induced by cTNF-α and cTGF-β/cIL-6 were thought to relate with various cytokines and several pathways activated by these cytokines, further study on signaling pathways was needed. Reduction of E-cadherin and expression of vimentin were also observed in edge of tumor in control group, which may be caused by secretion of cytokines from microenvironment. Further investigation of relationship between growth factor and cytokine-inducing EMT and tumor growth and metastasis was also thought to be needed.

Mouse transplanted model in this chapter showed tumor proliferation and metastatic forming in two mice by growth factor and cytokine stimulations, but replicated no clinical features of cIMC such as edema, hot feeling and pain. Two reports of mouse xenograft model of

hIBC and one of cIMC were issued. In all three reports, mice were xenografted with tissue fragments obtained from hIBC patients and cIMC dog. The emboli of tumor cells in lymph vessels and clinical features of inflammatory breast and mammary carcinoma were observed in all three reports (Alpaugh et al., 1999; Camacho et al., 2013; Shirakawa et al., 2001), whereas neither of them was observed in this study. Tissue fragments contained various cells such as cancer cells, stroma cells, immune cells and inflammatory cells, and cytokines secreted by these cells. They worked multiply and interact each other in microenvironment (Hanahan and Coussens, 2012). The reason why emboli of lymph vessels and inflammatory symptom were not observed in this mouse model, was thought to be lack or shortage of these cells and cytokines. For further investigation of EMT in cIMC in vivo experiment, it is needed to see which kinds of components are needed for replicate cIMC features in mouse model.

In this chapter, stimulations of growth factor and cytokine and their combinations promoted tumor proliferation and metastasis to lymph node and lung. From expression patterns of E-cadherin and vimentin in several lesions, center of tumor, lymph node and distant metastatic foci, EMT was suggested to be involved in tumor metastasis. However, evaluation of expression of EMT markers used in this study could not reveal the relationship between EMT and growth factor and cytokine-inducing tumor proliferations and acquisition of metastatic potential. Although this mouse model might be insufficient to replicate clinicopathology of

cIMC, this mouse model partially indicated that inflammatory cytokines progressed the malignancy of cMGT such as tumor proliferation and metastasis. In order to clarify the relationship between EMT induced by inflammatory stimulation and malignant progression of cMGT, further studies of the evaluation of much kind of EMT markers and down-stream factors which were activated by cytokines, were thought to be needed.

(a)

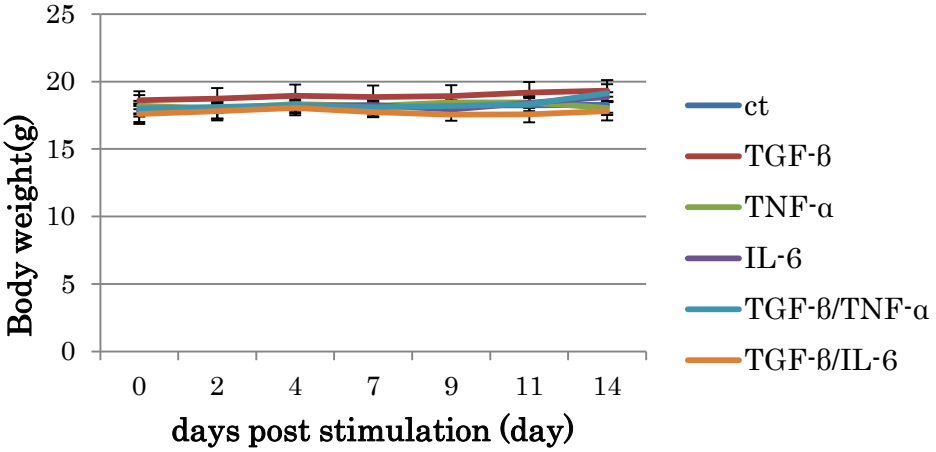

(b)

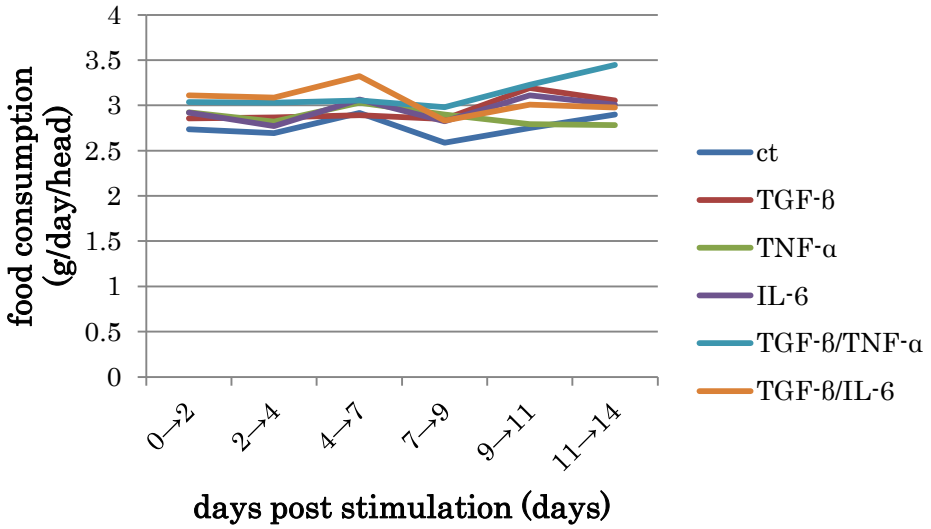

Fig.4.1 Body weight and food consumption of CIPp 4B transplanted mice.

(a)Body weights of mice were not significantly reduced by stimulations. (b)Food consumption also showed no changes. Vertical bar represents SE.

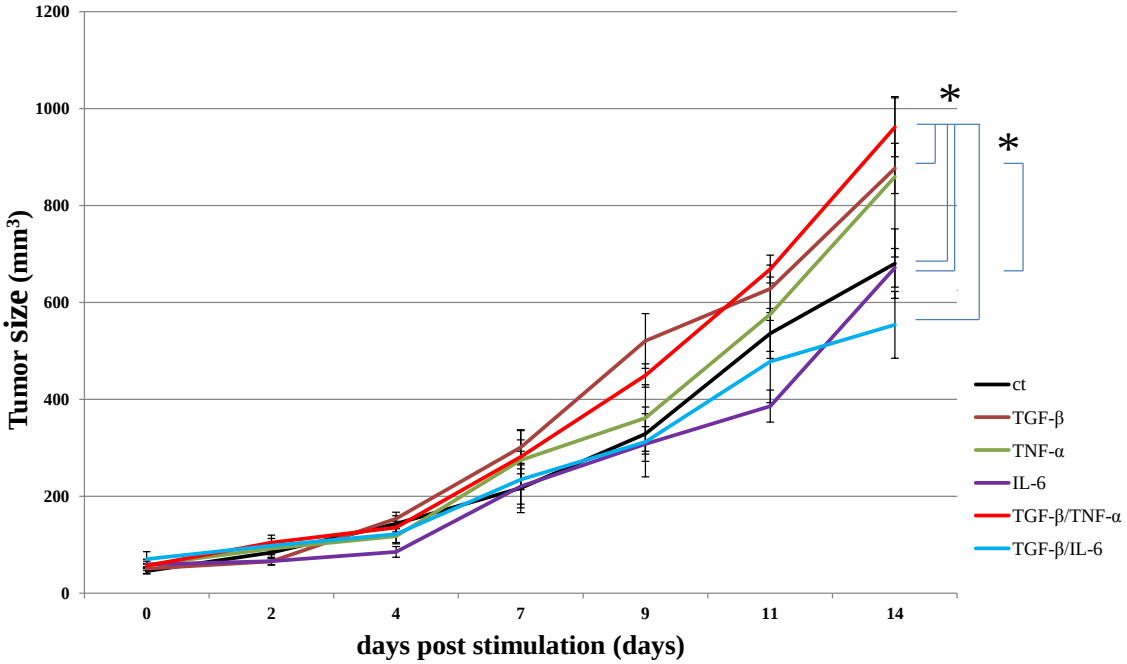

Fig.4.2 Comparisons of tumor sizes.

Average tumor sizes of each stimulation were compared. The cTGF-β stimulated mice were significantly larger than control mice at 14 days post stimulation. The cTGF-β/cTNF-α stimulated mice were significantly larger than control mice and the cTGF-β, cIL-6 cTGF-β/cIL-6 stimulated mice at 14 days post stimulation. ＊: $p < 0.05$. Vertical bar represents SE.

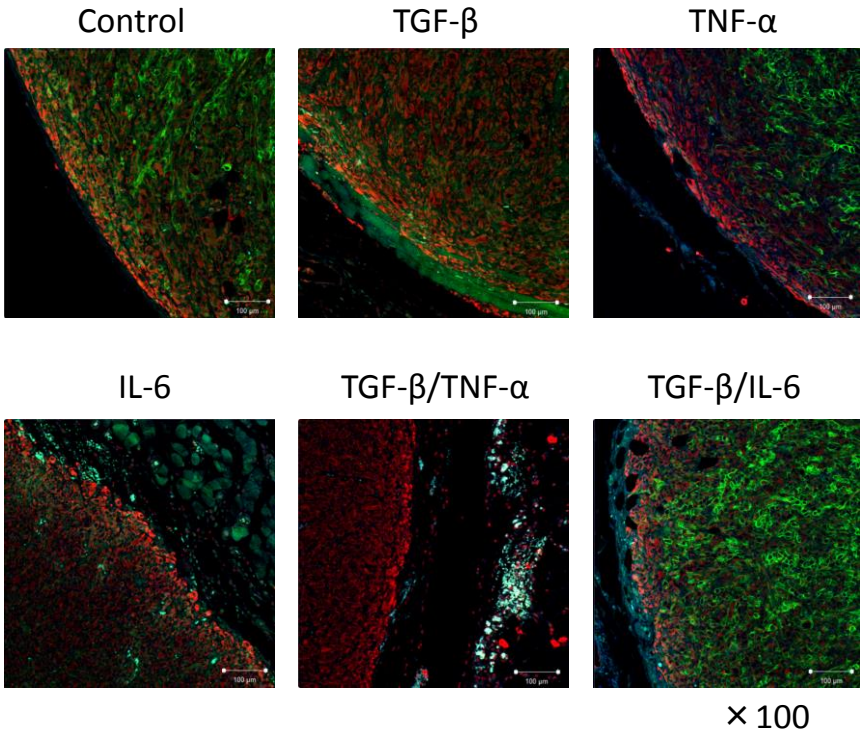

Fig.4.3 Localization of EMT marker on the edge of growing tumor.

Sections of tumor with each stimulation were fluorescently detected with anti-E-cadherin antibody and anti-vimentin antibody. On the edge of tumor, expressions of E-cadherin were low and expressions of vimentin were high in all tumors. Green: E-cadherin. Red: Vimentin. Blue: DAPI.

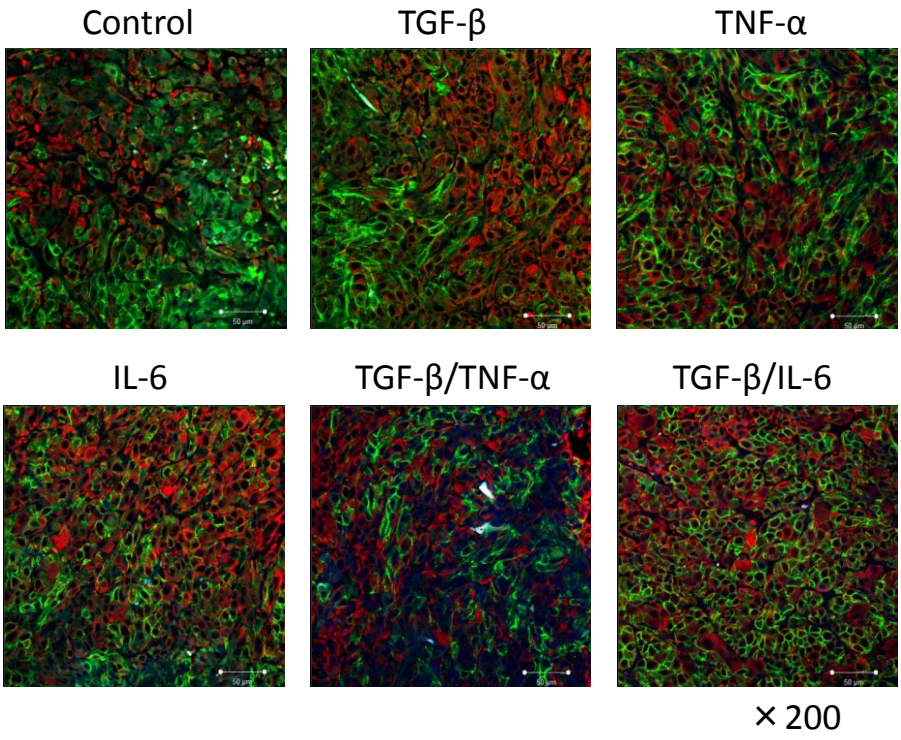

Fig.4.4 Localization of EMT marker in the center of tumor.

Sections of tumor with each stimulation were fluorescently detected with anti-E-cadherin antibody and anti-vimentin antibody. In the center of tumor, E-cadherin and vimentin were both expressed, but merges of both were rarely observed. Green: E-cadherin. Red: Vimentin. Blue: DAPI.

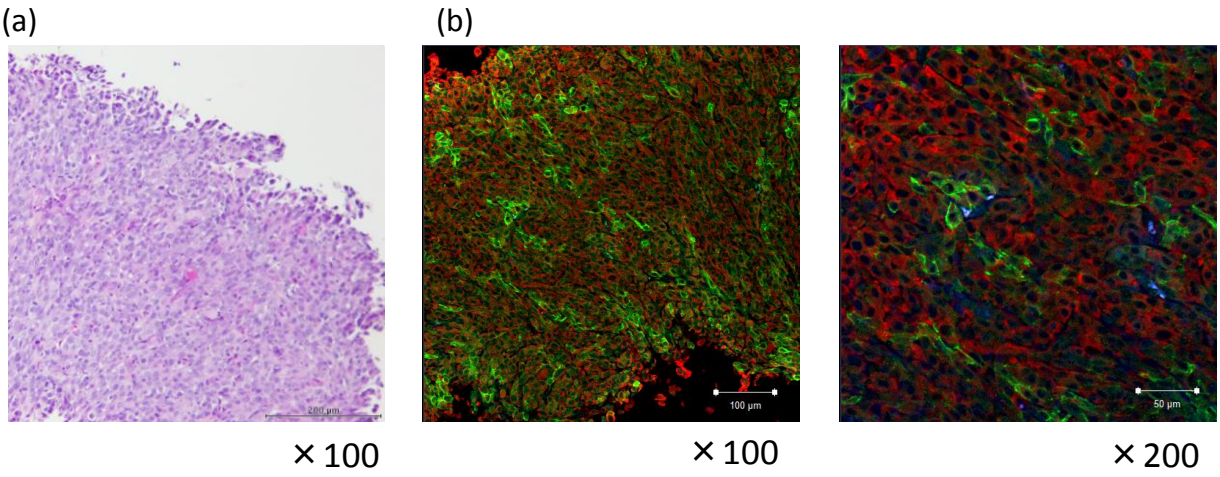

Fig.4.5 Lymph node metastasis.

(a)Lymph node metastasis was observed in cTNF-α stimulated mouse with hematoxylin-eosin stain. (b)Metastatic lesions were fluorescently detected with anti-E-cadherin antibody and anti-vimentin antibody. Tumor cells in metastatic lesions expressed both E-cadherin and vimentin, but merges of both were rarely observed like the center of primary lesions. Green: E-cadherin. Red: Vimentin. Blue: DAPI.

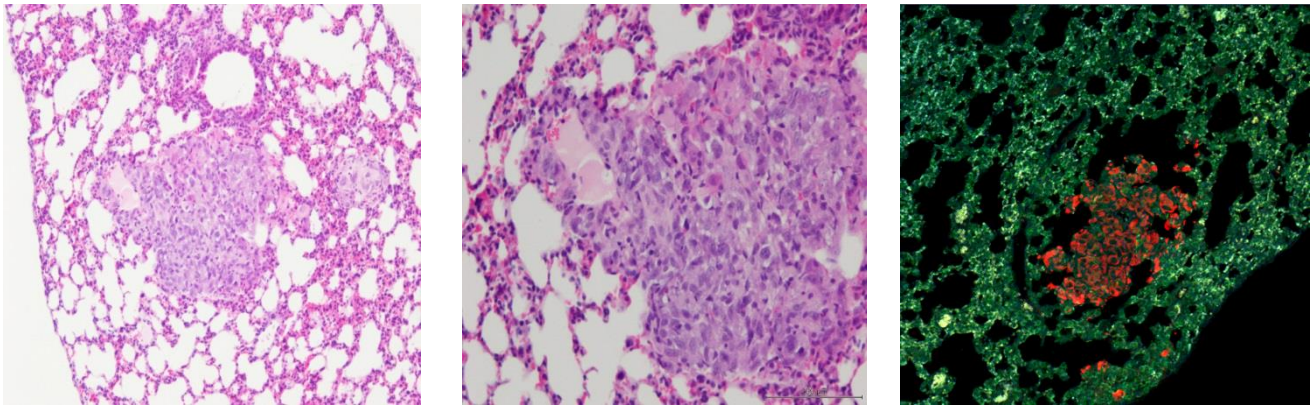

×100　　×200　　×100

Fig.4.6 Lung metastasis.

(a)Lung metastasis was observed in cTGF-β/cIL-6 stimulated mouse with hematoxylin-eosin stain. (b)Metastatic lesions were fluorescently detected with anti-E-cadherin antibody and anti-vimentin antibody. Tumor cells in metastatic lesions expressed both E-cadherin and vimentin, but merges of both were rarely observed like the center of primary lesions. Green: E-cadherin. Red: Vimentin. Blue: DAPI.

Summary

Canine IMC is one of the most malignant type of cMGT of which clinical features and prognosis are similar to hIBC (Marconato et al., 2009; Pérez-Alenza et al., 2001). In hIBC, EMT induced by inflammatory cytokines existed in tumor microenvironment is suspected to be affected its malignancy (Mohamed et al., 2014). Therefore, the malignancy of cIMC was thought to have relationship with EMT and inflammation. It was hypothesized that the malignancy of cMGT was associated with inflammation and EMT induced by inflammation. To prove this hypothesis, following studies ware performed in this study.

In chapter 1, to investigate EMT in cIMC in comparison to non-cIMC, evaluations of the expressions of epithelial and mesenchymal markers were performed. The average of EMT score of cIMC was significantly higher and score of EMT marker changes about E-cadherin, vimentin and fibronectin were significantly higher in cIMCs than in non-cIMCs. Although cytokeratin 18 was significantly reduced in non-cIMC in comparison to cIMC, fibronectin was significantly up-regulated in cIMC comparing to non-cIMC. The ratio of E-cadherin(-)/vimentin(+) cells was significantly higher in cIMC in comparison to non-cIMC. These results suggested that cIMC had closer relationship with EMT comparing to non-cIMC.

In chapter 2, because homology between human and dog is not extremely high and effects of this difference on canine cell lines were unclear, constructions and purifications of canine recombinant TGF-β, TNF-α and IL-6 and confirmations of their functions as EMT

inducing factors were performed for the following studies. These recombinant cytokines were confirmed by western blot analysis. Stimulation by these cytokines reduced or lost E-cadherin expressions in MDCK cells. Furthermore, stimulated MDCK cells lost cell-cell adhesions and changed their morphology. These alterations were features of EMT. Therefore, these cytokines showed the ability of EMT inducer.

In chapter 3 section 1, investigation of whether EMT was induced by stimulation with single and combination of canine recombinant cytokine TGF-β, TNF-α and IL-6 in six cMGT cell lines was performed. Cytokines and their combinations induced the changes of EMT markers in cMGT cell lines with various ways and degrees. These diversities of EMT marker changes were thought to be due to tumor heterogeneity. Canine MGT cell lines used in this section were derived from tumor tissue of spontaneous MGT cases and had not been cloned. The accumulation of different reactivities of each cell population against cytokine stimulation may mask the effects of cytokines on cMGT cell lines. To reveal the effects of cytokines on cMGT cell lines, cloning of a cMGT cell line was performed in section 2.

As tumors were reported to contain various phenotypes of cells (Kan et al., 2010), CIPp cell line was cloned into 11 clonal cell lines in section 2. The features of 11 clonal cell lines were evaluated by expressions of EMT markers. Among these clonal cell lines, CIPp-4b cell line showed nearly epithelial features such as high expression of E-cadherin, expression of

ZO-1 and low expression of fibronectin. Therefore, this cell line was selected and stimulated by recombinant cytokines. CIPp-4b cells showed expression changes of several EMT markers, and their changes were stronger in comparison to parental CIPp cells. These cytokines were suggested to induce EMT in CIPp-4b cell line *in vitro*. However, it was still unclear whether these EMT changes induced by growth factor and inflammatory cytokines reproduced the malignancy of cIMC including rapid tumor growth, distant and lymph node metastasis.

In chapter 4, to investigate whether EMT induced by growth factor and inflammatory cytokines reproduced the rapid proliferation and distant and lymph node metastasis of cIMC, CIPp-4b cells were transplanted into mice and stimulated with cytokines by local injection. The stimulation with cTGF-β and cTGF-β/cTNF-α significantly increased tumor size in comparison to control group. Furthermore, stimulations with cTNF-α and cTGF-β/cIL-6 promoted lymph node and lung metastasis, respectively. These results suggested that stimulations by these cytokines progressed tumor proliferation and metastasis. From expression patterns of E-cadherin in formed tumor and metastatic lesions, EMT was suggested to be involved in tumor metastasis. However, evaluation of expression of EMT markers used in this study could not reveal the relationship between EMT and growth factor and cytokine-inducing tumor proliferations and acquisition of metastatic potential. Although this mouse model might be insufficient to replicate clinicopathology of cIMC, this model could show that the malignant

progression of cMGT was caused by inflammatory stimulation.

In this study, EMT was suggested to be involved in cIMC, and recombinant cTGF-β, cTNF-α and cIL-6 were also suggested to induce EMT in cMGT cell line. Although these growth factor and inflammatory cytokines might promote tumor proliferation and metastasis through EMT, it was still unclear whether EMT was related to clinicopathological features of cIMC. For further investigation of revealing the relationship between EMT and the malignant progression of cMGT, analysis of expression patterns of more kinds of EMT markers and searching of signaling pathway associated with EMT were needed.

Acknowledgements

I would like to express the gratitude to my mentor, Professor Ryohei Nishimura, Department of Veterinary Surgery, Graduate School of Agricultural and Life Sciences, the University of Tokyo, for the excellent instructions, constructive suggestions and continuous encouragement.

Furthermore, I would like to appreciate my mentor, Emeritus Professor Nobuo Sasaki, Department of Veterinary Surgery, the University of Tokyo, and Professor Manabu Mochizuki, Department of Emergency Medicine, the University of Tokyo, for their detailed advises.

Besides, I would like to give special thanks to Assistant Professor Takayuki Nakagawa and Research Assistant Professor Naoki Fujita, Department of Veterinary Surgery, the University of Tokyo, for his great supports in all my studies.

Moreover, I would like to show my gratitude for provisions of tissue samples to Professor Hiroyuki Nakayama, Associate Professor Kazuyuki Uchida and Assistant Professor James Kenn Chambers, Department of Veterinary Pathology, the University of Tokyo, Associate Professor Hideo Akiyoshi, Department of Veterinary Clinical Science, Osaka Prefecture University, Lecturer Masaki Michishita, Department of Veterinary Pathology, Nippon Veterinary and Life Science University, and Dr. Yumiko Kagawa, Northlab.

Unforgettably, I would like to express the gratitude for provisions of canine RNA to Professor Hajime Tsujimoto and Dr. Takashi Tamamoto, Department of Internal Medicine, the University of Tokyo

Additionally, I would like to show my gratitude for provision of cell line to Associate Professor Taisuke Horimoto, Department of Veterinary Microbiology, the University of Tokyo.

I would like to thank all the members of Department of Veterinary Surgery, Department of Emergency Medicine and Veterinary Medical Center, The University of Tokyo for all supports.

Finally, I would like to thank my family for their outstanding support and encouragement.

References

Abulaiti, A., Shintani, Y., Funaki, S., Nakagiri, T., Inoue, M., Sawabata, N., Minami, M., and Okumura, M. (2013). Interaction between non-small-cell lung cancer cells and fibroblasts via enhancement of TGF-β signaling by IL-6. Lung Cancer *82*, 204–213.

Alpaugh, M.L., Tomlinson, J.S., Shao, Z., and Barsky, S.H. (1999). A Novel Human Xenograft Model of Inflammatory Breast Cancer Advances in Brief A Novel Human Xenograft Model of Inflammatory Breast Cancer. Cancer Res. *59*, 5079–5084.

Anderson, W.F., Schairer, C., Chen, B.E., Hance, K.W., and Levine, P.H. (2005). Epidemiology of Inflammatory Breast Cancer (IBC). Breast Dis. *22*, 9–23.

Asgeirsson, K.S., Olafsdóttir, K., Jónasson, J.G., and Ogmundsdóttir, H.M. (1998). The effects of IL-6 on cell adhesion and E-cadherin expression in breast cancer. Cytokine *10*, 720–728.

Bagnato, A., and Rosanò, L. (2007). Epithelial-mesenchymal transition in ovarian cancer progression: a crucial role for the endothelin axis. Cells. Tissues. Organs *185*, 85–94.

Balkwill, F. (2006). TNF-alpha in promotion and progression of cancer. Cancer Metastasis Rev. *25*, 409–416.

Balkwill, F.R. (2009). Tumour necrosis factor and cancer. Nat. Rev. Cancer *9*, 361–371.

Balkwill, F., and Mantovani, A. (2001). Inflammation and cancer: back to Virchow? Lancet *357*, 539–545.

Ben-Baruch, A. (2003). Inflammatory cells , cytokines and chemokines in breast cancer progression : reciprocal tumor – microenvironment interactions. Breast Cancer Res. *5*, 31–36.

Blanco, D., Vicent, S., Elizegi, E., Pino, I., Fraga, M.F., Esteller, M., Saffiotti, U., Lecanda, F., and Montuenga, L.M. (2004). Altered expression of adhesion molecules and epithelial-mesenchymal transition in silica-induced rat lung carcinogenesis. Lab. Invest. *84*, 999–1012.

Bonnomet, A., Syne, L., Brysse, A., Feyereisen, E., Thompson, E.W., Noël, A., Foidart, J.-M., Birembaut, P., Polette, M., and Gilles, C. (2012). A dynamic in vivo model of epithelial-to-mesenchymal transitions in circulating tumor cells and metastases of breast cancer. Oncogene *31*, 3741–3753.

Brabletz, T., Jung, A., Reu, S., Porzner, M., Hlubek, F., Kunz-Schughart, L.A., Knuechel, R., and Kirchner, T. (2001). Variable beta-catenin expression in colorectal cancers indicates tumor progression driven by the tumor environment. Proc. Natl. Acad. Sci. U. S. A. *98*, 10356–10361.

Brodey, R.S., Goldschmidt, M.H., and Roszel, J.R. (1983). Canine mammary-gland neoplasms. J. Am. Anim. Hosp. Assoc. *19*, 61–90.

Brown, K.A., Aakre, M.E., Gorska, A.E., Price, J.O., Eltom, S.E., Pietenpol, J.A., and Moses, H.L. (2004). Induction by transforming growth factor-beta1 of epithelial to mesenchymal transition is a rare event in vitro. Breast Cancer Res. *6*, R215–R231.

Camacho, L., Peña, L., González Gil, A., Cáceres, S., Díez, L., and Illera, J.C. (2013). Establishment and characterization of a canine xenograft model of inflammatory mammary carcinoma. Res. Vet. Sci. *95*, 1068–1075.

Casas, E., Kim, J., Bendesky, A., Ohno-Machado, L., Wolfe, C.J., and Yang, J. (2011). Snail2 is an essential mediator of Twist1-induced epithelial mesenchymal transition and metastasis. Cancer Res. *71*, 245–254.

Charafe-Jauffret, E., Tarpin, C., Bardou, V.-J., Bertucci, F., Ginestier, C., Braud, A.-C., Puig, B., Geneix, J., Hassoun, J., Birnbaum, D., et al. (2004). Immunophenotypic analysis of inflammatory breast cancers: identification of an "inflammatory signature". J. Pathol. *202*, 265–273.

Chen, C., Zimmermann, M., Tinhofer, I., Kaufmann, A.M., and Albers, A.E. (2013). Epithelial-to-mesenchymal transition and cancer stem(-like) cells in head and neck squamous cell carcinoma. Cancer Lett. *338*, 47–56.

Christiansen, J.J., and Rajasekaran, A.K. (2006). Reassessing epithelial to mesenchymal transition as a prerequisite for carcinoma invasion and metastasis. Cancer Res. *66*, 8319–8326.

Clemente, M., Pérez-Alenza, M.D., and Peña, L. (2010a). Metastasis of canine inflammatory versus non-inflammatory mammary tumours. J. Comp. Pathol. *143*, 157–163.

Clemente, M., Pérez-Alenza, M.D., Illera, J.C., and Peña, L. (2010b). Histological, immunohistological, and ultrastructural description of vasculogenic mimicry in canine mammary cancer. Vet. Pathol. *47*, 265–274.

Coussens, L.M., Zitvogel, L., and Palucka, A.K. (2013). Neutralizing Tumor-Promoting Chronic Inflammation : A Magic Bullet ? Science (80-.). *339*, 286–292.

Dawood, S., Merajver, S.D., Viens, P., Vermeulen, P.B., Swain, S.M., Buchholz, T.A., Dirix, L.Y., Levine, P.H., Lucci, A., Krishnamurthy, S., et al. (2011). International expert panel on inflammatory breast cancer: consensus statement for standardized diagnosis and treatment. Ann. Oncol. *22*, 515–523.

Diakos, C.I., Charles, K.A., McMillan, D.C., and Clarke, S.J. (2014). Cancer-related inflammation and treatment effectiveness. Lancet Oncol. *15*, e493–e503.

Egenvall, A., Bonnett, B.N., Ohagen, P., Olson, P., Hedhammar, A., and von Euler, H. (2005). Incidence of and survival after mammary tumors in a population of over 80,000 insured female dogs in Sweden from 1995 to 2002. Prev. Vet. Med. *69*, 109–127.

Fernandez, S. V, Robertson, F.M., Pei, J., Aburto-Chumpitaz, L., Mu, Z., Chu, K., Alpaugh, R.K., Huang, Y., Cao, Y., Ye, Z., et al. (2013). Inflammatory breast cancer (IBC): clues for targeted therapies. Breast Cancer Res. Treat. *140*, 23–33.

Fernandez-Garcia, B., Eiró, N., Marín, L., González-Reyes, S., González, L.O., Lamelas, M.L., and Vizoso, F.J. (2014). Expression and prognostic significance of fibronectin and matrix metalloproteases in breast cancer metastasis. Histopathology *64*, 512–522.

Fernando, R.I., Castillo, M.D., Litzinger, M., Hamilton, D.H., and Palena, C. (2011). IL-8 signaling plays a critical role in the epithelial-mesenchymal transition of human carcinoma cells. Cancer Res. *71*, 5296–5306.

Fuxe, J., and Karlsson, M.C.I. (2012). TGF-β-induced epithelial-mesenchymal transition: a link between cancer and inflammation. Semin. Cancer Biol. *22*, 455–461.

Gao, J., Zhu, Y., Nilsson, M., and Sundfeldt, K. (2014). TGF-β isoforms induce EMT independent migration of ovarian cancer cells. Cancer Cell Int. *14*, 72.

Gilbertson, S.R., Kurzman, I.D., Zachrau, R.E., Hurvitz, A.I., and Black, M.M. (1983). Canine mammary epithelial neoplasms:biologic implications of morphologic characteristics assessed in 232 dods. Vet. Pathol. *20*, 127–142.

Goto-Koshino, Y., Ohno, K., Nakajima, M., Mochizuki, H., Kanemoto, H., and Tsujimoto, H. (2011). A rapid and simple method to obtain canine peripheral blood-derived macrophages. J. Vet. Med. Sci. *73*, 773–778.

Hanahan, D., and Coussens, L.M. (2012). Accessories to the crime: functions of cells recruited to the tumor microenvironment. Cancer Cell *21*, 309–322.

Ho, M.-Y., Tang, S.-J., Chuang, M.-J., Cha, T.-L., Li, J.-Y., Sun, G.-H., and Sun, K.-H. (2012). TNF-α induces epithelial-mesenchymal transition of renal cell carcinoma cells via a GSK3β-dependent mechanism. Mol. Cancer Res. *10*, 1109–1119.

Itoh, T., Uchida, K., Ishikawa, K., Kushima, K., Kushima, E., Tamada, H., Moritake, T., Nakao, H., and Shii, H. (2005). Clinicopathological Survey of 101 Canine Mammary Gland Tumors : Differences between Small-Breed Dogs and Others. J. Vet. Med. Sci. *67*, 345–347.

Just, U., Stocking, C., Spooncer, E., Dexter, T.M., and Ostertag, W. (1991). Expression of the GM-CSF gene after retroviral transfer in hematopoietic stem cell lines induces synchronous granulocyte-macrophage differentiation. Cell *64*, 1163–1173.

Kalluri, R., and Weinberg, R.A. (2009). The basics of epithelial-mesenchymal transition. J. Clin. Invest. *119*, 1420–1428.

Kamitani, S., Yamauchi, Y., Kawasaki, S., Takami, K., Takizawa, H., Nagase, T., and Kohyama, T. (2011). Simultaneous stimulation with TGF-β1 and TNF-α induces epithelial mesenchymal transition in bronchial epithelial cells. Int. Arch. Allergy Immunol. *155*, 119–128.

Kan, Z., Jaiswal, B.S., Stinson, J., Janakiraman, V., Bhatt, D., Stern, H.M., Yue, P., Haverty, P.M., Bourgon, R., Zheng, J., et al. (2010). Diverse somatic mutation patterns and pathway alterations in human cancers. Nature *466*, 869–873.

Kawata, M., Koinuma, D., Ogami, T., Umezawa, K., Iwata, C., Watabe, T., and Miyazono, K. (2012). TGF-β-induced epithelial-mesenchymal transition of A549 lung adenocarcinoma cells is enhanced by pro-inflammatory cytokines derived from RAW 264.7 macrophage cells. J. Biochem. *151*, 205–216.

Kim, J.-H., Im, K.-S., Kim, N.-H., Chon, S.-K., Doster, A.R., and Sur, J.-H. (2011). Inflammatory mammary carcinoma with metastasis to the brain and distant organs in a spayed Shih Tzu dog. J. Vet. Diagnostic Investig. *23*, 1079–1082.

Kleer, C.G., Golen, K.L. Van, Braun, T., and Merajver, S.D. (2001). Persistent E-Cadherin Expression in Inflammatory Breast Cancer. Mod. Pathol. *14*, 458–464.

Kokkinos, M.I., Wafai, R., Wong, M.K., Newgreen, D.F., Thompson, E.W., and Waltham, M. (2007). Vimentin and epithelial-mesenchymal transition in human breast cancer -observations in vitro and in vivo. Cells. Tissues. Organs *185*, 191–203.

Kudo-Saito, C., Shirako, H., Takeuchi, T., and Kawakami, Y. (2009). Cancer metastasis is accelerated through immunosuppression during Snail-induced EMT of cancer cells. Cancer Cell *15*, 195–206.

Lamouille, S., Xu, J., and Derynck, R. (2014). Molecular mechanisms of epithelial-mesenchymal transition. Nat. Rev. Mol. Cell Biol. *15*, 178–196.

Lerebours, F., Vacher, S., Andrieu, C., Espie, M., Marty, M., Lidereau, R., and Bieche, I. (2008). NF-kappa B genes have a major role in inflammatory breast cancer. BMC Cancer *8*.

Levine, P.H., Portera, C.C., Hoffman, H.J., Yang, S.X., Takikita, M., Duong, Q.N., Hewitt, S.M., and Swain, S.M. (2012). Evaluation of lymphangiogenic factors, vascular endothelial growth factor D and E-cadherin in distinguishing inflammatory from locally advanced breast cancer. Clin. Breast Cancer *12*, 232–239.

Li, C.-W., Xia, W., Huo, L., Lim, S.-O., Wu, Y., Hsu, J.L., Chao, C.-H., Yamaguchi, H., Yang, N.-K., Ding, Q., et al. (2012). Epithelial-mesenchymal transition induced by TNF-α requires NF-κB-mediated transcriptional upregulation of Twist1. Cancer Res. *72*, 1290–1300.

Li, Q., Liu, B.-C., Lv, L.-L., Ma, K.-L., Zhang, X.-L., and Phillips, A.O. (2011). Monocytes induce proximal tubular epithelial-mesenchymal transition through NF-kappa B dependent upregulation of ICAM-1. J. Cell. Biochem. *112*, 1585–1592.

Li, W., Zhang, B., Li, H., Zhao, C., Zhong, Y., Sun, J., and Lv, S. (2014). TGF β1 mediates epithelial mesenchymal transition via β6 integrin signaling pathway in breast cancer. Cancer Invest. *32*, 409–415.

Liu, X. (2008). Inflammatory cytokines augments TGF-beta1-induced epithelial-mesenchymal transition in A549 cells by up-regulating TbetaR-I. Cell Motil. Cytoskeleton *65*, 935–944.

Liu, T., Zhang, X., Shang, M., Zhang, Y., Xia, B., Niu, M., Liu, Y., and Pang, D. (2013). Dysregulated expression of Slug, vimentin, and E-cadherin correlates with poor clinical outcome in patients with basal-like breast cancer. J. Surg. Oncol. *107*, 188–194.

Marconato, L., Romanelli, G., Stefanello, D., Giacoboni, C., Bonfanti, U., Bettini, G., Finotello, R., and Verganti, S. (2009). Prognostic factors for dogs with mammary inflammatory carcinoma : 43 cases (2003 – 2008). Jounal Am. Vet. Med. Assoc. *235*, 967–972.

Miettinen, P.J., Ebner, R., Lopez, A.R., and Derynck, R. (1994). TGF-β induced transdifferentiation of mammary epithelial cells to mesenchymal cells: involvement of type I receptors. Jounal Cell Biol. *127*, 2021–2036.

Misdorp, W., Else, R.W., Hellmen, E., and Lipscomb, T.P. (1999). Histological Classification of Mammary Tumors of the Dog and Cat, 2nd ser., vol. 7. Armed Forces Inst. Pathol. Coop. with Am. Regist. Pathol. World Heal. Organ. Collab. Cent. Worldw. Ref. Comp. Oncol. Washington, DC.

Mohamed, M.M., El-Ghonaimy, E.A., Nouh, M.A., Schneider, R.J., Sloane, B.F., and El-Shinawi, M. (2014). Cytokines secreted by macrophages isolated from tumor microenvironment of inflammatory breast cancer patients possess chemotactic properties. Int. J. Biochem. Cell Biol. *46*, 138–147.

Morales, J., and Alpaugh, M.L. (2009). Gain in cellular organization of inflammatory breast cancer: A 3D in vitro model that mimics the in vivo metastasis. BMC Cancer *9*.

Morali, O.G., Delmas, Â., Moore, R., Jeanney, C., Thiery, J.P., and Larue, L. (2001). IGF-II induces rapid b -catenin relocation to the nucleus during epithelium to mesenchyme transition. Oncogene *20*, 4942–4950.

Morel, A.-P., Hinkal, G.W., Thomas, C., Fauvet, F., Courtois-Cox, S., Wierinckx, A., Devouassoux-Shisheboran, M., Treilleux, I., Tissier, A., Gras, B., et al. (2012). EMT inducers catalyze malignant transformation of mammary epithelial cells and drive tumorigenesis towards claudin-low tumors in transgenic mice. PLoS Genet. *8*, e1002723.

Morita, T., Mayanagi, T., and Sobue, K. (2007). Dual roles of myocardin-related transcription factors in epithelial mesenchymal transition via slug induction and actin remodeling. J. Cell Biol. *179*, 1027–1042.

Moyano, J. V, Greciano, P.G., Buschmann, M.M., Koch, M., and Matlin, K.S. (2010). Autocrine transforming growth factor-β1 activation mediated by integrin αVβ3 regulates transcriptional expression of laminin-332 in madin-darby canine kidney epithelial cells. Mol. Biol. Cell *21*, 3654–3668.

Nakaya, Y., and Sheng, G. (2013). EMT in developmental morphogenesis. Cancer Lett. *341*, 9–15.

Nicolás, F.J., Lehmann, K., Warne, P.H., Hill, C.S., and Downward, J. (2003). Epithelial to mesenchymal transition in Madin-Darby canine kidney cells is accompanied by down-regulation of Smad3 expression, leading to resistance to transforming growth factor-beta-induced growth arrest. J. Biol. Chem. *278*, 3251–3256.

Olmeda, D., Jordá, M., Peinado, H., Fabra, a, and Cano, a (2007). Snail silencing effectively suppresses tumour growth and invasiveness. Oncogene *26*, 1862–1874.

Peña, L., Nieto, A., Perez-Alenza, M.D., Rodriguez, A., Sanchez, M.A., and Castaño, M. (1994). Expression of fibronectin and its integrin receptor alpha 5 beta 1 in canine mammary tumours. Res. Vet. Sci. *57*, 358–364.

Peña, L., Perez-alenza, M.D., Rodriguez-bertos, A., and Nieto, A. (2003). Canine inflammatory mammary carcinoma : histopathology , immunohistochemistry and clinical implications of 21 cases. Breast Cancer Res. Treat. *78*, 141–148.

Peppicelli, S., Bianchini, F., and Calorini, L. (2014). Inflammatory cytokines induce vascular endothelial growth factor-C expression in melanoma-associated macrophages and stimulate melanoma lymph node metastasis. Oncol. Lett. *8*, 1133–1138.

Pérez-Alenza, M.D., Tabanera, E., and Peña, L. (2001). Inflammatory mammary carcinoma in dogs : 33 cases (1995 – 1999). Jounal Am. Vet. Med. Assoc. *219*, 1110–1114.

Polette, M., Mestdagt, M., Bindels, S., Nawrocki-Raby, B., Hunziker, W., Foidart, J.-M., Birembaut, P., and Gilles, C. (2007). Beta-catenin and ZO-1: shuttle molecules involved in tumor invasion-associated epithelial-mesenchymal transition processes. Cells. Tissues. Organs *185*, 61–65.

Rismanchi, S., Yadegar, O., Muhammadnejad, S., Amanpour, S., Taghizadeh-Jahed, M., and Muhammadnejad, A. (2014). Expression of vimentin filaments in canine malignant mammary gland tumors: A simulation of clinicopathological features of human breast cancer. Biomed. Reports *2*, 725–728.

Rokavec, M., Öner, M.G., Li, H., Jackstadt, R., Jiang, L., Lodygin, D., Kaller, M., Horst, D., Ziegler, P.K., Schwitalla, S., et al. (2014). IL-6R/STAT3/miR-34a feedback loop promotes EMT-mediated colorectal cancer invasion and metastasis. J. Clin. Invest. *124*, 1853–1867.

Sarli, G., Preziosi, R., Tolla, L.D., Brunetti, B., and Benazzi, C. (2004). E-Cadherin Immunoreactivity in Canine Mammary Tumors. J. Vet. Diagnostic Investig. *16*, 542–547.

Shirakawa, K., Tsuda, H., and Heike, Y. (2001). Absence of Endothelial Cells , Central Necrosis , and Fibrosis Are Associated with Aggressive Inflammatory Breast Cancer Advances in Brief. Cancer Res. *61*, 445–451.

Souza, C.H.D.M., Toledo-piza, E., Amorin, R., Barboza, A., and Tobias, K.M. (2009). Inflammatory mammary carcinoma in 12 dogs: Clinical features, cyclooxygenase-2 expression, and response to piroxicam treatment. Can. Vet. J. *50*, 506–510.

Sullivan, N.J., Sasser, A.K., Axel, A.E., Vesuna, F., Raman, V., Ramirez, N., Oberyszyn, T.M., and Hall, B.M. (2009). Interleukin-6 induces an epithelial-mesenchymal transition phenotype in human breast cancer cells. Oncogene *28*, 2940–2947.

Thiery, J.P. (2002). Epithelial-mesenchymal transitions in tumour progression. Nat. Rev. Cancer *2*, 442–454.

Thiery, J.P., Acloque, H., Huang, R.Y.J., and Nieto, M.A. (2009). Epithelial-mesenchymal transitions in development and disease. Cell *139*, 871–890.

Tsai, J.H., and Yang, J. (2013). Epithelial-mesenchymal plasticity in carcinoma metastasis. Genes Dev. *27*, 2192–2206.

Tsuji, T., Ibaragi, S., and Hu, G. (2009). Epithelial-mesenchymal transition and cell cooperativity in metastasis. Cancer Res. *69*, 7135–7139.

Uyama, R., Nakagawa, T., Hong, S.-H., Mochizuki, M., Nishimura, R., and Sasaki, N. (2006). Establishment of four pairs of canine mammary tumour cell lines derived from primary and metastatic origin and their E-cadherin expression. Vet. Comp. Oncol. *4*, 104–113.

Vieira, P., de Waal-Malefyt, R., Dang, M.N., Johnson, K.E., Kastelein, R., Fiorentino, D.F., deVries, J.E., Roncarolo, M.G., Mosmann, T.R., and Moore, K.W. (1991). Isolation and expression of human cytokine synthesis inhibitory factor cDNA clones: homology to Epstein-Barr virus open reading frame BCRFI. Proc. Natl. Acad. Sci. U. S. A. *88*, 1172–1176.

Vora, H., Patel, N., Rajvik, K., Mehta, S., Brahmbhatt, B., Shah, M., Shukla, S., and Shah, P. (2009). Cytokeratin and vimentin expression in breast cancer. Int. J. Biol. Markers *24*, 38–46.

Wang, H., Fang, R., Wang, X.-F., Zhang, F., Chen, D.-Y., Zhou, B., Wang, H.-S., Cai, S.-H., and Du, J. (2013a). Stabilization of Snail through AKT/GSK-3β signaling pathway is required

for TNF-α-induced epithelial-mesenchymal transition in prostate cancer PC3 cells. Eur. J. Pharmacol. *714*, 48–55.

Wang, H., Wang, H.-S., Zhou, B.-H., Li, C.-L., Zhang, F., Wang, X.-F., Zhang, G., Bu, X.-Z., Cai, S.-H., and Du, J. (2013b). Epithelial-mesenchymal transition (EMT) induced by TNF-α requires AKT/GSK-3β-mediated stabilization of snail in colorectal cancer. PLoS One *8*, e56664.

Weitzenfeld, P., Meron, N., Leibovich-rivkin, T., Meshel, T., and Ben-baruch, A. (2013). Progression of Luminal Breast Tumors Is Promoted by Ménage à Trois between the Inflammatory Cytokine TNFα and the Hormonal and Growth-Supporting Arms of the Tumor Microenvironment. Mediators Inflamm.

Weng, Y.-R., Cui, Y., and Fang, J.-Y. (2012). Biological functions of cytokeratin 18 in cancer. Mol. Cancer Res. *10*, 485–493.

Willipinski-Stapelfeldt, B., Riethdorf, S., Assmann, V., Woelfle, U., Rau, T., Sauter, G., Heukeshoven, J., and Pantel, K. (2005). Changes in cytoskeletal protein composition indicative of an epithelial-mesenchymal transition in human micrometastatic and primary breast carcinoma cells. Clin. Cancer Res. *11*, 8006–8014.

Woelfle, U., Sauter, G., Santjer, S., Brakenhoff, R., and Pantel, K. (2004). Down-Regulated Expression of Cytokeratin 18 Promotes Progression of Human Breast Cancer. Clin. Canser Res. *10*, 2670–2674.

Xu, J., Lamouille, S., and Derynck, R. (2009). TGF-beta-induced epithelial to mesenchymal transition. Cell Res. *19*, 156–172.

Yadav, A., Kumar, B., Datta, J., Teknos, T.N., and Kumar, P. (2011). IL-6 promotes head and neck tumor metastasis by inducing epithelial-mesenchymal transition via the JAK-STAT3-SNAIL signaling pathway. Mol. Cancer Res. *9*, 1658–1667.

Yang, C.-C., and Wolf, D.A. (2009). Inflamed snail speeds metastasis. Cancer Cell *15*, 355–357.

Yang, J., Mani, S.A., Donaher, J.L., Ramaswamy, S., Itzykson, R.A., Come, C., Savagner, P., Gitelman, I., Richardson, A., Weinberg, R.A., et al. (2004). Twist , a Master Regulator of Morphogenesis , Plays an Essential Role in Tumor Metastasis. Cell *117*, 927–939.

Yoshida, K., Yoshida, S., Choisunirachon, N., Saito, T., Matsumoto, K., Saeki, K., Mochizuki, M., Nishimura, R., Sasaki, N., and Nakagawa, T. (2014). The Relationship between

Clinicopathological Features and Expression of Epithelial and Mesenchymal Markers in Spontaneous Canine Mammary Gland Tumors. J. Vet. Med. Sci. *76*, 1321–1327.

Zhang, A., Dong, Z., and Yang, T. (2006). Prostaglandin D2 inhibits TGF-beta1-induced epithelial-to-mesenchymal transition in MDCK cells. Am. J. Physiol. Renal Physiol. *291*, F1332–F1342.

Zhang, J., Tian, X.-J., Zhang, H., Teng, Y., Li, R., Bai, F., Elankumaran, S., and Xing, J. (2014). TGF-β-induced epithelial-to-mesenchymal transition proceeds through stepwise activation of multiple feedback loops. Sci. Signal. *7*, ra91.